Chen (Referee)

Interactive comment on "Impacts of short-term mitigation measures on $PM_{2.5}$ and radiative effects: a case study from a regional background site near Beijing, China" by Qiyuan Wang et al.

This study was conducted in a regional background site near Beijing during the 19th National Congress of the Communist Party of China. The authors investigated the effectiveness of short-term mitigation measures on $PM_{2.5}$ and aerosol direct radiative forcing. They found that $PM_{2.5}$ mass and its sources are reduced significantly during the control period compared with the non-control period. Those decreases in aerosol concentration in turn, as shown by the climate radiative effect estimates, alleviated aerosol cooling effects. Moreover, the authors further analyzed two pollution episodes after control period based on the WRF-Chem model. This is an interesting study. I believe that this paper makes a useful contribution to the literature and could be published in ACP after a minor revision in response to the following suggestions (see specific comments below).

Response: The authors appreciate the reviewer for his or her valuable time to review our manuscript.

Specific Comments:

1. In section 2.2.1: the authors should give the storage condition of the samples.

Response: We have added information concerning storage conditions for the samples in the revised manuscript. It now reads: "To minimize the evaporation of volatile materials, the samples were stored in a refrigerator at -4 °C before the chemical analyses."

2. Page 8, Line 11-13: It should be noted that the equation (12) is based on the assumption of no contribution from brown carbon, a light-absorbing organic matter. It should be pointed out this in the article.

Response: Following the reviewer's suggestion, we revised the text to read: "A second assumption for this part of the study was that there was negligible absorption by brown carbon in the visible region (Yang et al., 2009), and on this basis, the b_{abs} can be determined from the EC mass concentration using linear regression (Eq. 12)."

3. Section 3.1: This study analyzed data from a single site near Beijing, even though it included detail chemical and optical measurements. The emission control for NCCPC control period included a wide range of measures and could impact the air quality for a lager domain. Therefore, it would be more convincing if the authors could also include measurements for surrounding areas from other platforms, such as the AERONET AODs and satellite aerosol retrievals.

Response: Although the AERONET AODs are helpful for providing a spatial distribution of aerosols in Beijing-Tianjin-Hebei (BTH) region, the observation periods were limited, typically at ~10:30 and 13:30 local time. Another complicating factor is

that relative humidity can have an important influence on AODs. After careful consideration, we concluded that it is more useful to focus on $PM_{2.5}$ concentrations at different locations in BTH region to illustrate the effectiveness of the control measures. As shown in Figure S3 (revised supporting information, also see Figure R1 below), the $PM_{2.5}$ concentrations over much of the BTH region showed a decreasing trend during the NCCPC-control period compared with the non-control period. In the revised manuscript, we added the following text: "Meanwhile, the PM2.5 mass concentrations obtained from the China Environmental Monitoring Center also showed a decreasing trend over most of the BTH region during the NCCPC-control period (see Figure S3)."

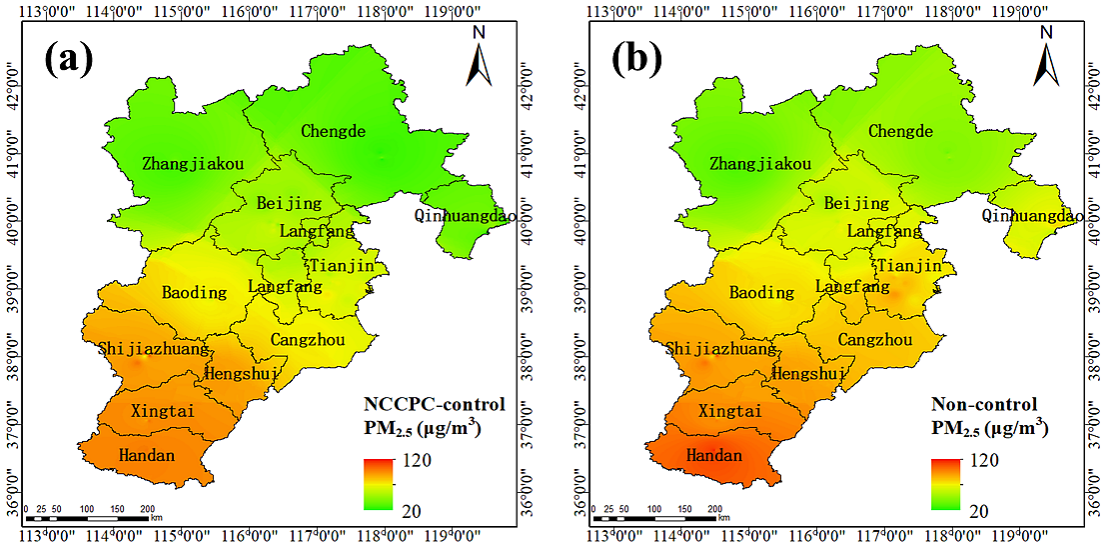

Figure R1. Spatial distribution of $PM_{2.5}$ mass concentration in Beijing-Tianjin-Hebei region during the (a) 19th National Congress of the Communist Party of China (NCCPC) control period and (b) non-control period.

4. About the light scattering construction of the particles (Sec 3.4, "Impacts of $PM_{2.5}$ emission reduction on aerosol radiative effects"), the reconstructed b_{scat} shows some deviation from the estimated b_{scat} values. What is the reason for the difference?

Response: Although the IMPROVE-based method provides reasonable estimates of the chemical b_{scat} in this study, the lack of locally-derived mass scattering efficiency information is a probable reason for the ~10% underestimates of measured values. In the revised manuscript, we revised the text, which now reads: "This result indicates that the IMPROVE-based method provided a good estimation of the chemical b_{scat}; nonetheless, it is likely that more locally-measured mass scattering efficiencies for each chemical species could reduce the underestimates of measured values."

5. The paper must be polished and edited for English grammar and word usage before it can be published in ACP.

Response: Our revised manuscript has been polished by a native English speaker.

Please see our new manuscript.

Anonymous Referee #2

Interactive comment on "Impacts of short-term mitigation measures on $PM_{2.5}$ and radiative effects: a case study from a regional background site near Beijing, China" by Qiyuan Wang et al.

General comments

This manuscript attempts to examine the impacts of emission reduction on $PM_{2.5}$ and radiative effects (surface DRF as the authors defined) using field measurements and WRF-Chem simulations at a regional background station in the Beijing-Tianjin- Hebei region in China. The impacts are examined by comparing the changes in observation-derived speciated $PM_{2.5}$ concentrations and DRF during and after an emission-controlled period. The paper is reasonably written and results are reasonably presented, and it can be accept for publishing with revisions that address the following issues.

Response: The authors appreciate the reviewer's thoughtful and valuable suggestions, and we believe that the revised manuscript has been significantly improved after considering his or her comments. Below are point-to-point responses.

A major weakness in the study is that, as the main objective is to investigate the impacts of emission reduction measure on $PM_{2.5}$ and DRF (emphasized in the title and abstract), this paper has a major flaw in separating the effects of emission reduction and meteorological conditions. Although the authors make an effort to make comparisons between the during- and-post-control periods under stable meteorological conditions, the determination of the "stable" conditions is quite rough, and it is not clear how similar the meteorological conditions are for the days selected for the comparison (even under stable conditions, the degree of the stability would significantly affect air quality). To separate these two factors, I would suggest the authors to do a more thorough analysis of the meteorological conditions, or ideally, based on the information they have and/or can obtain, construct an emission reduction scenario for the NCCPC control period and conduct additional WRF-Chem simulations and analysis.

Response: The reviewer correctly points out that variations in the mass concentrations of $PM_{2.5}$ and its chemical composition can be caused by a variety of factors, including meteorological conditions as well as emission sources. We agree with the reviewer that it would be desirable to construct an emission reduction scenario for the NCCPC-control period and then perform additional WRF-Chem simulations and analyses. Unfortunately, it was not possible for us to obtain detailed information concerning the reduction measures taken by the government, and therefore we could not develop an accurate emission inventory for the NCCPC-control period.

As an alternative, we compared days during the control and non-control periods with stable atmospheric conditions because that was a way to evaluate particle accumulation when the effects of transport would be minimal. Furthermore, because the duration of the control period was not long, it was not possible to precisely match meteorological conditions to investigate reduction in $PM_{2.5}$ during NCCPC-control and non-control period. Although "stable conditions" were empirically defined for our study, the general idea of minimizing meteorological influences was helpful for evaluating the

effectiveness of the emission control measures. We focused on wind speed and mixed layer height because they are important factors in determining the horizontal and vertical dispersion of particles.

As shown in Figure 3 (also see Figure R1 below) in the revised manuscript, the relationships between $PM_{2.5}$ concentrations and wind speed and mixed layer height can be fitted with power functions. Our strategy was to use the inflection points of the power functions as a way to identify stable atmospheric conditions. The average wind speeds and mixed layer heights were lower under stable atmospheric conditions during the NCCPC-control period than the non-control period, indicating that particles may have been more prone to accumulate during the NCCPC-control period. This means that if there had been no effective control measures during the NCCPC-period, the mass concentrations of $PM_{2.5}$ likely would have been higher compared with the days under stable atmospheric condition during the non-control period, but this was not the case. Thus, we think that the "stable atmospheric condition" approach is still useful for evaluating the effectiveness of the control measures.

Moreover, we now include surface weather charts in revised Figure S5 (also see Figure R2 below) to compare and contrast the weather conditions during the days with stable atmospheric conditions during the control and non-control periods. Finally, following the reviewer's suggestion, we include a more in-depth analysis of the meteorological conditions in the revised manuscript. The text now reads: "There were two days for the NCCPC-control period and three days for the non-control period that satisfied the stability criteria. The surface charts (Figure S5) show that the weather conditions for those selected stable atmosphere days during the NCCPC-control and non-control periods were mainly controlled by uniform pressure fields and weak low-pressure systems, respectively, and those conditions led to weak or calm surface winds. Due to the lower WS (0.2 versus 0.3 m s^{-1}) and MLH (213 versus 244 m) during the NCCPC-control period relative to the non-control period, the horizontal and vertical dispersion for the stable atmospheric days were slightly weaker during the NCCPC-control period. As shown in Table 1, the percent differences for $PM_{2.5}$ (43.4%), NO3- (25.9%), OM (68.1%), EC (40.0%), and fine soil (58.7%) were larger for the days with stable atmospheric conditions compared with those for all days. These results are a further indication that the control measures were effective in reducing pollution, but meteorology also influenced the aerosol pollution."

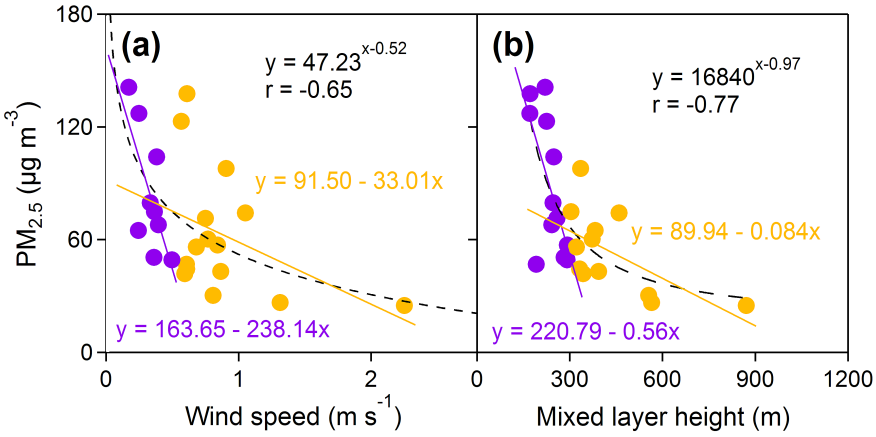

Figure R1. Scatter plots showing the relationships between $PM_{2.5}$ mass concentrations and (a) wind speed and (b) mixed layer height.

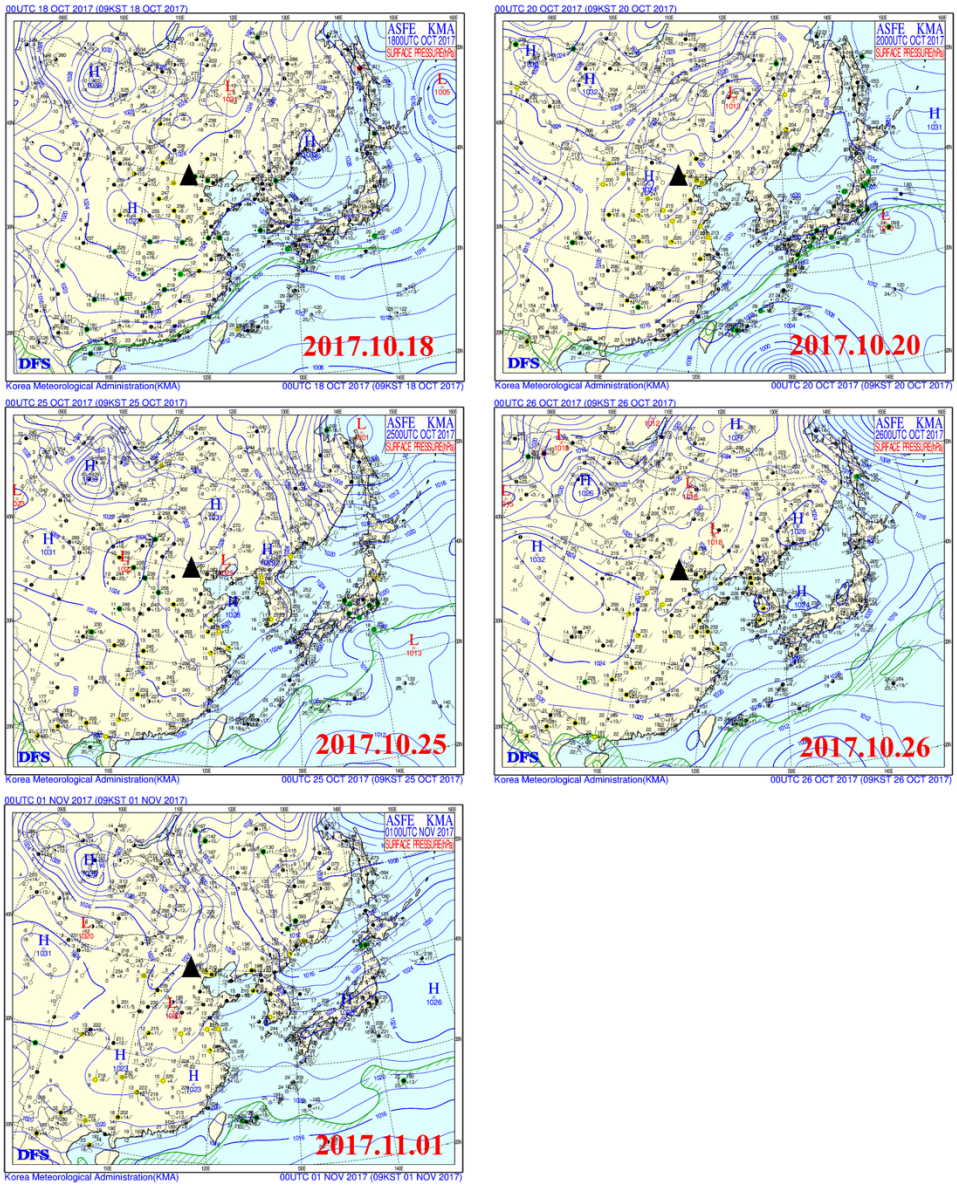

Figure R2. Surface weather charts for 08:00 (local time) over East Asia during the five

days with stable atmospheric conditions. The black triangles represent Xianghe.

Another issue is about the source apportionment in Section 3.2 using PMF. The authors assign the third source factor to secondary inorganic aerosols (SIA). This is not appropriate, since SIA is not an emission source, and it may have contributions from other sources they identify, such as coal combustion, mobile, industry, and biomass burning, i.e., SIA is not independent to other four identified anthropogenic emissions sources.

Response: In the broadest terms, $PM_{2.5}$ originates from primary sources (e.g., coal combustion, traffic emissions, industry, and biomass burning) and secondary processes, that is, the formation of particles through homogeneous reactions in the atmosphere. As the reviewer correctly noted, secondary inorganic aerosol forms from precursors emitted by primary sources. Receptor models (e.g., PMF) generally cannot resolve the sources for secondary particles, and therefore, we now classify this factor as "secondary particle formation" in the revised manuscript.

Specific comments
1. Page 8, line 13. It is better to show the regression results, and specify the values of a and b used.

Response: Following the reviewer's suggestion, we added the following in the revised manuscript: "As shown in Figure S2, the derived slope (a) and intercept (b) for the regression model were 10.8 m^2 g^{-1} and -4.7, respectively."

2. Page 9, lines 52-54. Small changes in sulfates may also be attributed to small changes in SO_2 emissions during the campaign.

Response: Yes, in addition to the low SO_2 concentrations throughout the campaign, the change in SO_2 concentration during the NCCPC-control (8.5 µg m^{-3}) versus non-control period (12.4 µg m^{-3}) was small. Following the reviewer's suggestion, we revised the original explanation to "However, SO_4^{2-} exhibited similar loadings during the NCCPC-control (5.8 µg m^{-3}) and non-control (5.3 µg m^{-3}) periods. This is consistent with the small differences in SO_2 concentrations for the NCCPC-control (8.5 µg m^{-3}, Figure S4) versus the non-control (12.4 µg m^{-3}, Figure S4) periods. Indeed, the low SO_2 concentrations may not have provided sufficient gaseous precursors to form substantial amounts of sulfate."

3. Figures 4 and 5. Copy the source legend from Fig 5 to Fig 4.

Response: Change made. Please see our revised Figure 4 in the revised manuscript.

4. Page 10, lines 64 -72. First, as pointed earlier, the approach to determine the "stable conditions" is rough. Second, the samples (3 days and 2 days) for the stable conditions are too small, which would make the comparison statistically no meaningful. A better analysis is needed to separate the impacts of emission reduction and meteorological conditions.

Response: As noted above, it has not been possible for us to obtain the emission inventory for the NCCPC control period. Therefore, our analysis of relatively stable atmospheric conditions was the best approach we had for evaluating the effectiveness of control measures. As the control measures were only in place for a short amount of time, this comparison is limited but it does support the argument that control measures were effective. We note in the revised manuscript that results of other studies also have shown short-term emission controls reduced pollutant levels, so our results were not unexpected. Following the reviewer's suggestion, we added more analysis of the meteorological conditions in the revised manuscript. Please see our response above.

5. Page 15, lines 42-43. It is surprising that with an averaged surface concentration of 6.0ug/m3, EC imposes the largest cooling effects in surface DRF during the non-control period and several factors higher than that of OM, while the light extinction by OM is much higher than by EC. An explanation would be helpful.

Response: The concentration of EC was 6.0 $\mu g/m^3$, and the light absorption caused by EC accounted for 14.3% of light extinction coefficient. The large contribution of EC absorption may be attributed enhancements caused by internal mixing with other materials because that process has been shown to amplify the light absorption of EC. In the revised manuscript, we added the following explanation: "The high EC DRF may have been due in part to EC particles internally mixed with other materials because mixing can amplify light absorption and thereby increase DRF."

6. Fig 8 seems too small and a little bit complicated, which make it difficult to the reader to understand the effects of meteorological conditions on air quality in the BTH area. In addition, the location of the Xianghe site should be specified in the figure. Similar figure for October 12-23 might also be needed when you do analysis in decomposing the influences of the emission reduction and meteorology (especially for the five "stable" days).

Response: Following the reviewer's suggestion, we modified the Figure 8 (also see Figure R3 below) in the revised manuscript. Moreover, the surface weather charts for the five "stable" days were added in the revised supporting information. Please see the response above.

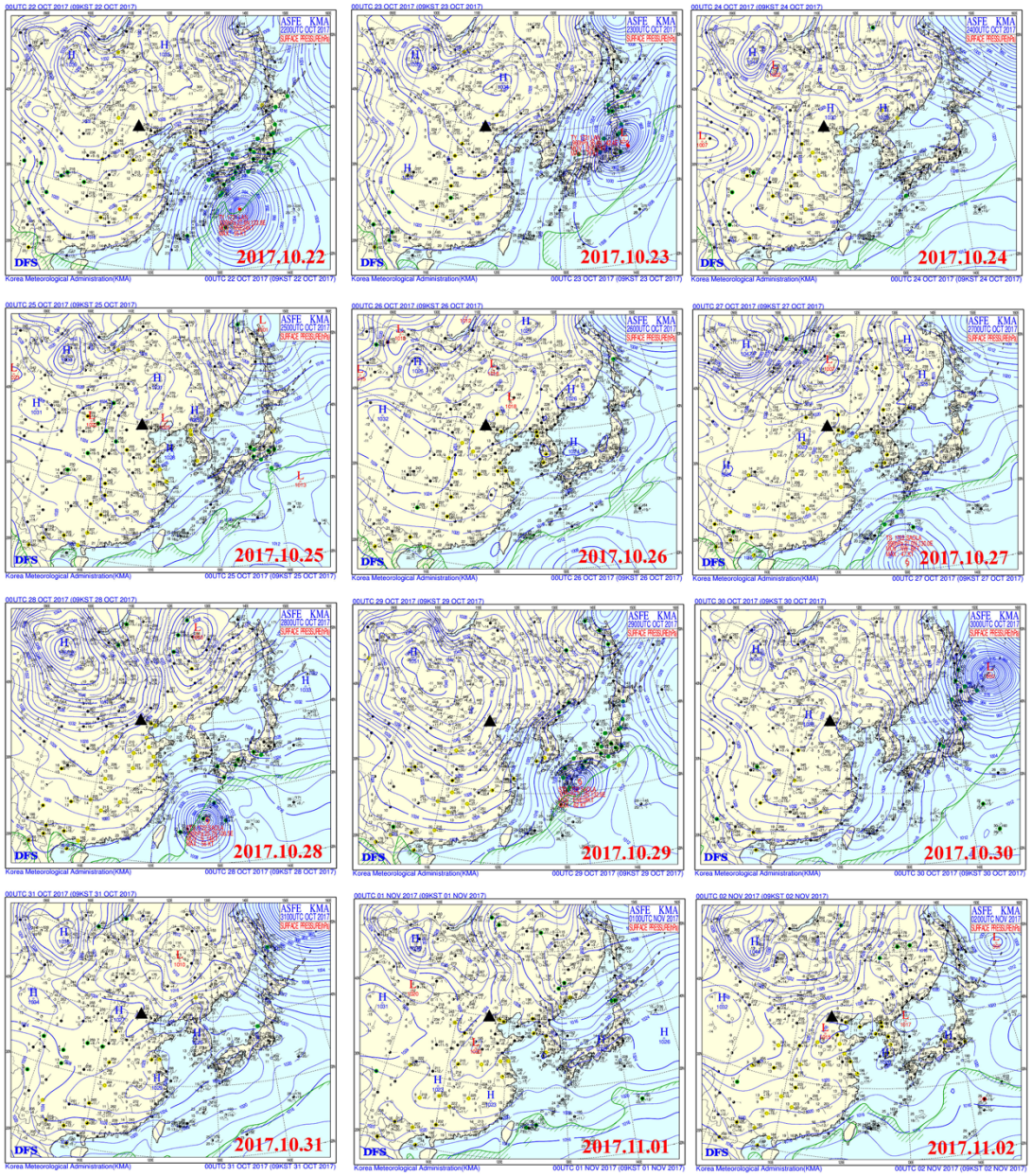

Figure R3. Surface weather patterns at 08:00 (local time) over East Asia from 22 October to 2 November 2017. The black triangle represents Xianghe.

Technical
The language need to be polished. The authors need go through the manuscript carefully and make edits. Following are just a few pickups.

Response: The revised manuscript was polished by a native English speaker. Please see our new manuscript.

Page 2 line 35, page 15 line 46, page 17 line 82: change "would" to "should"? Page 2 line 44, change "experienced" to "experiencing"?

Response: Change made.

Page 3 line 78, change "low-voltage" to "low-pressure".

Response: Change made.

Page 14 line 88, "genesis"?

Response: In the revised manuscript, we revised our original expression to "The calculated mean bias and RMSE for $PM_{2.5}$ were -6.8 and 32.8 μg m^{-3}, and the index of agreement was 0.75, indicating that the formation of $PM_{2.5}$ during the two pollution episodes was reasonably well captured by the WRF-Chem model even though the predicted average $PM_{2.5}$ mass concentration of was lower than the observed value."

Impacts of short-term mitigation measures on $PM_{2.5}$ and radiative effects: case study at a regional background site near Beijing, China

Qiyuan Wang[1*], Suixin Liu[1], Nan Li[2], Wenting Dai[1], Yunfei Wu[3], Jie Tian[4], Yaqing Zhou[1], Meng Wang[1], Steven Sai Hang Ho[1], Yang Chen[5], Renjian Zhang[3], Shuyu Zhao[1], Chongshu Zhu[1], Yongming Han[1,6], Xuexi Tie[1], Junji Cao[1,7*]

[1]Key Laboratory of Aerosol Chemistry and Physics, State Key Laboratory of Loess and Quaternary Geology, Institute of Earth Environment, Chinese Academy of Sciences, Xi'an, 710061, China.
[2]School of Environmental Science and Engineering, Nanjing University of Information Science & Technology, Nanjing, 210044, China
[3]Key Laboratory of Regional Climate-Environment Research for Temperate East Asia, Institute of Atmospheric Physics, Chinese Academy of Sciences, Beijing, 100029, China.
[4]Department of Environmental Science and Engineering, School of Energy and Power Engineering, Xi'an Jiaotong University, Xi'an 710049, China.
[5]Chongqing Institute of Green and Intelligent Technology, Chinese Academy of Sciences, Chongqing 400714, China.
[6]School of Human Settlements and Civil Engineering, Xi'an Jiaotong University, Xi'an, 710049, China.
[7]Institute of Global Environmental Change, Xi'an Jiaotong University, Xi'an, 710049, China.

Correspondence to: Qiyuan Wang (wangqy@ieecas.cn) and Junji Cao (cao@loess.llqg.ac.cn)

Abstract. Measurements at a background site near Beijing showed that pollution controls implemented during the 19th National Congress of the Communist Party of China (NCCPC) were effective in reducing $PM_{2.5}$. Mass concentrations of $PM_{2.5}$ and its major chemical components were 20.6–43.1% lower during the NCCPC-control period compared with a non-control period, and differences were greater on days with stable meteorological conditions. A receptor model showed that $PM_{2.5}$ from traffic-related emissions, biomass burning, industry processes, and mineral dust was 38.5–77.8% lower during the NCCPC-control versus non-control period, but differences in $PM_{2.5}$ from coal burning were small, and secondary particle formation was higher during the control period. During one pollution episode in the non-control period, secondary inorganic aerosol dominated, and the WRF-Chem model showed that the Beijing-Tianjin-Hebei (BTH) region contributed 73.6% of $PM_{2.5}$ mass. A second pollution episode was linked to biomass burning, and BTH contributed 46.9% of $PM_{2.5}$ mass. Calculations based on IMPROVE algorithms showed that organic matter was the largest contributor to light extinction during the non-control period whereas NH_4NO_3 was the main contributor during the NCCPC. The Tropospheric Ultraviolet and Visible radiation model showed that the average direct radiative forcing (DRF) values at the Earth's surface were -14.0 and -19.3 W m^{-2} during the NCCPC-control and non-control periods, respectively, and the DRF for the individual $PM_{2.5}$ components were 22.7–46.7% lower during the NCCPC. The information and dataset

删除的内容: **a …ase study from** ... [1]

删除的内容: An intensive m…easurements at campaign was conducted in … regional …ackground site near Beijing showed that pollution controls implemented during the 19th National Congress of the Communist Party of China (NCCPC) wereto investigate the…effectiveness…of short-term mitigation measures on…n reducing $PM_{2.5}$ and aerosol direct radiative forcing (DRF)… Average m…ass concentrations of $PM_{2.5}$ and its major chemical composition …omponents wereare…decreased by …0.6 … …3.1% lower during the NCCPC …CCPC-control period compared with the … non-control period. … and differences were greater on When considering …ays with the…stable meteorological conditions, … larger reduction of $PM_{2.5}$ is found compared with that for all days. Further, …a…positive matrix factorization …eceptor model shows …howed that the mass concentrations of …$M_{2.5}$ from traffic-related emissions, biomass burning, industry processes, and mineral dust are …asreduced by…38.5 … …7.8% lower during the NCCPC …CCPC-control period …ersuscompared with the…non-control period. … but However, there is no significant …ifferences in $PM_{2.5}$ from coal burning were small, and between these two periods, and an increasing trend of $PM_{2.5}$ mass from …econdary particle formation was higher inorganic aerosol is found …uring the NCCPC …ontrol period. During oneTwo…pollution episode in the non-control period,s were occurred subsequently after the NCCPC control period. One is dominated by…secondary inorganic aerosol dominated, and the WRF-Chem model shows …howed that the Beijing-Tianjin-Hebei (BTH) region contributes …ontributed 73.6% of $PM_{2.5}$ mass; … A second pollution episode was linked tothe other is mainly caused by…biomass burning, and the …TH region …ontributes… 46.9% of $PM_{2.5}$ mass. Calculations based on a revised …MPROVE method …lgorithms showed that organic matter (OM) is…as the largest contributor to the…light extinction coefficient (b_{ext}) …uring the non-control period while …hereas NH_4NO_3 is …as the dominant …ain contributor during the NCCPC control period… The Tropospheric Ultraviolet and Visible radiation model reveals …howed that the average direct radiative forcing (DRF) values at the Earth's surface are …ere -14.0 and -19.3 W m^{-2} during the NCCPC …CCPC-control and non-control periods, respectively, and the reduction ratios of …RF for the individual due to the decrease in…$PM_{2.5}$ components vary from…ere 22.7 … …6.7% lower during the NCCPC control period… Our study would further provide valuable ... [2]

from this study will be useful for developing air pollution control strategies in the BTH region and for understanding associated aerosol radiative effects.

1 Introduction

High loadings of fine particulate matter ($PM_{2.5}$, particulate matter with an aerodynamic diameter ≤ 2.5 μm) cause air quality to deteriorate (Pui et al., 2014; Tao et al., 2017), reduce atmospheric visibility (Watson, et al., 2002; Cao et al., 2012), and adversely affect human health (Feng et al., 2016; Xie et al., 2016). Moreover, $PM_{2.5}$ can directly and indirectly affect climate and ecosystems (Lecoeur et al., 2014; Tie et al., 2016). With the rapid increases in economic growth, industrialization, and urbanization in the past two decades, Beijing has experienced serious $PM_{2.5}$ pollution, especially in winter (e.g., Zhang et al., 2013; Elser et al., 2016; Wang et al., 2016a; Zhong et al., 2018). Since the Chinese government promulgated the National Ambient Air Quality Standards for $PM_{2.5}$ in 2012 (NAAQS, GB3095–2012), a series of emission control strategies have been implemented in Beijing and surrounding areas to alleviate the serious air pollution problems. These measures include installing desulphurization systems in coal-fired power plants, banning high-emission motor vehicles, and promoting natural gas as an alternative to coal in rural areas. According to the China Environmental State Bulletin (www.zhb.gov.cn/hjzl/zghjzkgb/lnzghjzkgb, in Chinese), the annual levels of $PM_{2.5}$ during 2013–2016 in Beijing showed a decreasing trend (r = 0.98 and slope = -5.3 μg m^{-3} $year^{-1}$), but there were still 45.9% of days in 2016 that suffered from varying degrees of pollution.

Identifying the causes of air pollution in Beijing is challenging because the chemical composition of $PM_{2.5}$ is variable and complex, and the particles originate from a variety of sources and processes. For example, Elser et al. (2016) reported that organic aerosol (OA) was the largest contributor to $PM_{2.5}$ mass during extreme haze periods in Beijing, and the primary aerosol from coal combustion (46.8%) was the dominant contributor to OA, followed by the oxygenated OA (25.0%) and biomass burning OA (13.8%). In addition, Zheng et al. (2016) found that organic matter (OM) was the most abundant component (18–60%) in $PM_{2.5}$, and its relative contribution usually decreased as pollution levels rose while those of secondary inorganic species (e.g, sulfate and nitrate) increased.

In recent years, the Chinese government has taken temporary control measures to ensure good air quality during some important conferences and festivals held in Beijing, including the 2008 Summer Olympic Games, the 2014 Asia-Pacific Economic Cooperation (APEC) summit, and the 2015 Victory Day parade (VDP). These actions provide valuable opportunities for evaluating the effectiveness of emission controls

删除的内容：to help controlling…the …ir pollution control strategies in the BTH region and for understanding associated alleviating the cooling effects of …erosols at the surface in Beijing ... [3]

删除的内容：can strongly deteriorate…ause air quality to deteriorate (Pui et al., 2014; Tao et al., 2017), reduce atmospheric visibility (Watson, et al., 2002; Cao et al., 2012), and cause …dversely ae…fects to…human health (Feng et al., 2016; Xie et al., 2016). Moreover, $PM_{2.5}$ also …an directly andor…indirectly affect climate and ecosystems (Lecoeur et al., 2014; Tie et al., 2016). With the rapid increases in economic growth, industrialization, and urbanization in the past two decades, Beijing has been…experienced serious $PM_{2.5}$ pollution, especially in winter (e.g., Zhang et al., 2013; Elser et al., 2016; Wang et al., 2016a; Zhong et al., 2018). Since the Chinese government promulgated the new…National Ambient Air Quality Standards for $PM_{2.5}$ in 2012 (NAAQS, GB3095–2012) for $PM_{2.5}$ in 2012… a series of emission control strategies have been implementedperformed…in Beijing and its…surrounding areas to alleviate the serious air pollution problems, … These measures includee.g.…installing strong …esulphurization systems in coal-fired power plants, eliminating …anning high- …mission motor vehicles, and promoting natural gas as an alternative toinstead of…coal in rural areas. According to the data issued by the …hina Environmental State Bulletin (www.zhb.gov.cn/hjzl/zghjzkgb/lnzghjzkgb, in Chinese), although …he annual levels of $PM_{2.5}$ during 2013–2016 in Beijing shows …howed a decreasing trend (r = 0.98 and slope = -5.3 μg m^{-3} $year^{-1}$), but there are …ere still 45.9% of days in 2016 that suffering …uffered from different ... [4]

删除的内容：T…e causes of air pollution in Beijing are …s challenging becausecomplicated due to…the complex …hemical composition in …f $PM_{2.5}$ is variable and complex, and the particles originate from a variety of sources andtheir different formation…processes. For example, Elser et al. (2016) have …eported that organic aerosol (OA) is …as the largest contributor to $PM_{2.5}$ mass during the…extreme haze periods in Beijing, and the primary aerosol from coal combustion (46.8%) is …as the dominant contributor to OA, followed by the oxygenated OA (25.0%),…and biomass burning OA (13.8%). In contrast…ddition, Zheng et al. (2016) have …ound that organic matter (OM) is …as the most abundant component (18–60%) in ... [5]

删除的内容：usually …as taken takes some …emporary control measures to ensure good air quality duringfor…some important conferences or …nd festivals held in Beijing, e.g.…ncluding the,…2008 Summer Olympic Games, the 2014 Asia-Pacific Economic Cooperation (APEC) summit, and the 2015 Victory Day parade (VDP). These actions provide valuable opportunity …pportunities to …or evaluatinge ... [6]

on air pollution, and the information gathered during the control periods should useful for making policy decisions. Numerous studies have demonstrated that temporary aggressive control measures were effective in reducing primary pollutants and secondary aerosol formation in Beijing (e.g., Wang et al., 2010; Guo et al., 2013; Li et al., 2015; Tao et al., 2016; Xu et al., 2017).

Air pollution in Beijing is not only influenced by local emissions and the regional transport of pollutants but also by meteorological conditions (e.g., Li and Han, 2016; Bei et al., 2017). In this regard, Zhong et al. (2018) concluded that heavy pollution episodes in Beijing can be generally divided into two phases (1) a transport stage, which is characterized by increases in pollutants mainly transported from the south of Beijing and (2) an accumulation stage, during which there is dramatic growth in $PM_{2.5}$ loadings due to stagnant meteorological conditions. Moreover, several studies have shown that the emission controls put in place during important events were effective in decreasing aerosol concentrations, but meteorological conditions also played an important role in determining aerosol loadings (Gao et al., 2011; Liang et al., 2017). For example, Liang et al. (2017) have found that meteorological conditions and emission control measures had comparable impacts on $PM_{2.5}$ loadings in Beijing during the 2014 APEC (30% versus 28%, respectively) and the 2015 VDP (38% versus 25%).

The existing studies on the effects of temporary air pollution controls in Beijing have not covered mid-autumn when meteorological conditions are typically complex and variable. Indeed, Zhang et al. (2018) reported that two weather patterns common in October caused heavy pollution episodes in Beijing. One episode was linked a Siberian high-pressure system and a uniform high-pressure field while the second was associated with a cold front and a low-pressure system. For this study, measurements were made at a regional background site in the Beijing-Tianjin-Hebei (BTH) region to investigate the changes of $PM_{2.5}$ during the 19th National Congress of the Communist Party of China (NCCPC), which was held in Beijing from 18–24 October. Temporary control measures were implemented in Beijing and neighboring areas; these included restrictions on the number of vehicles, prohibition of construction activities, and restrictions on factories and industrial production. The primary objectives of this study were to (1) investigate the effectiveness of emission control measures on $PM_{2.5}$ and the associated changes in its chemical composition; (2) determine the contributions of emission sources to $PM_{2.5}$ mass during the NCCPC-control and non-control periods; and (3) evaluate the impacts of reductions of $PM_{2.5}$ on aerosol direct radiative forcing (DRF) at the Earth's surface. The study produced a valuable dataset and the results provide insights into how controls on air pollution can affect Beijing.

删除的内容: which is certainly great value …or makingfuture…policy decisionsmaking… Numerous studies have demonstrated that the…temporary aggressive control measures are …ere efficient ... [7]

删除的内容: Furthermore…oreover, several studies have used …hown that the emission controls put in place during important events were effective models to quantify the contributions of pollution control strategies and meteorological conditions …n decreasing aerosol concentrationsreducing pollutants… and they indicate that although the emission controls are effective in decreasing aerosol concentrations,…ut the…meteorological conditions also played an important role in producing low…etermining aerosol loadings (Gao et al., 2011; Liang et al., 2017). For example, Liang et al. (2017) have found that meteorological conditions and emission control measures have …ad comparable impacts oncontributions in reducing ... [8]

删除的内容: Autumn is a transition season between summer and winter and always has…complex and variable meteorological conditions… Indeed,For example,…Zhang et al. (2018) have …eported that two typical …eather patterns common in October caused heavy pollution episodes in Beijing. One episode was linked aof the…Siberian high and uniform …igh-pressure system and a uniform high-pressure field while the second was associated with aand the…cold front and a low-voltage …ressure system play important roles in causing heavy pollution episodes in Beijing in October… Up to now, although plenty of studies have investigated the effectiveness of rigorous regulations on air pollutants in Beijing during the Olympics, APEC, and VDP, there are still lack of investigations made in mid-autumn (e.g., October). In…or this study, a series of …easurements were performed …ade atin…a regional background site in the Beijing-Tianjin-Hebei (BTH) region to investigate the changes of $PM_{2.5}$ during the 19th National Congress of the Communist Party of China (NCCPC), which was held in Beijing during …rom 18–24 October. Some t…emporary control measures were implemented in Beijing and neighboring areas; these included(e.g.,…restrictions oning…the number of vehicles, prohibition ofng…construction activities, and shutting …estrictions ondown part of…factories or …nd restricting …ndustrial production) were implemented in Beijing and its vicinity… Consequently, t…hehe…primary objectives of this study are …ere(1)…to (1) investigate the effectiveness of emission control measures on $PM_{2.5}$ and the associated changes in its chemical composition; (2) to…determine the contributions of emission sources to $PM_{2.5}$ mass during the NCCPC …CCPC-control and non-control periods; and (3) to…evaluate the impacts of reductions of $PM_{2.5}$ on the …erosol direct radiative forcing (DRF) at the Earth's surface. This …he study would ... [9]

2 Materials and methods

2.1 Sampling site

Intensive measurements were made from 12 October to 4 November 2017 at the Xianghe Atmospheric Observatory (39.75° N, 116.96° E; 36 m above sea level) to investigate how the characteristics of $PM_{2.5}$ and the associated radiative effects were affected by the controls put in place during the NCCPC. Xianghe is a small county with 0.33 million residents, and it is located in a major plain-like area ~50 km southeast from Beijing and ~70 km north from Tianjin (Figure 1). The sampling site is surrounded by residential areas and farmland, and it is ~5 km west of Xianghe city center. This regional aerosol background site is influenced by mixed emission sources in the BTH region. A more detailed description of the site may be found in Ran et al. (2016).

2.2 Measurements

2.2.1 Offline measurements

$PM_{2.5}$ samples were collected on 47 mm quartz-fiber filter (QM/A; GE Healthcare, Chicago, IL, USA) and Teflon® filters (Whatman Limited, Maidstone, UK) using two parallel mini-volume samplers (Airmetrics, Oregon, USA) that operated at a flow rate of 5 L min^{-1}. The duration of sampling was 24 h, and the sampling interval was from 09:00 local time to 09:00 the next day. To minimize the evaporation of volatile materials, the samples were stored in a refrigerator at -4 °C before the chemical analyses. The quartz-fiber filters were used for determinations of water-soluble inorganic ions and carbonaceous species, while the Teflon® filters were used for inorganic elemental analyses. The $PM_{2.5}$ mass on each sample filter was determined gravimetrically using a Sartorius MC5 electronic microbalance with ± 1 μg sensitivity (Sartorius, Göttingen, Germany). For the mass determinations, the filters were equilibrated under controlled temperature (20–23 ºC) and relative humidity (35–45%) before the measurements were made. Field blanks (a blank quartz-fiber filter and a blank Teflon® filter) were collected and analysed to account for possible background effects.

Water-soluble inorganic ions, including F^-, Cl^-, NO_3^-, SO_4^{2-}, Na^+, K^+, Mg^{2+}, Ca^{2+}, and NH_4^+ were measured with the use of a Dionex 600 ion chromatograph (IC, Dionex Corp., Sunnyvale, CA, USA). The four anions of interest were separated using an ASII-HC column (Dionex Corp.) and 20 mM potassium hydroxide as the eluent. The five cations were separated with a CS12A column (Dionex) and an eluent of 20 mM methane sulfonic acid. More detailed description of the IC analyses may be found in Zhang et al. (2011). Carbonaceous species, including organic carbon (OC) and elemental carbon (EC)

删除的内容: conducted
删除的内容: a.s.l.
删除的内容: its
删除的内容: period
删除的内容: .
删除的内容: I
删除的内容: and is
已移动(插入) [1]
删除的内容: observation site is a
删除的内容: that
删除的内容: from
已上移 [1]: The sampling site is surrounded by residential areas and farmland and is ~5 km west of Xianghe city center.
删除的内容: M
删除的内容: Oregon
删除的内容: analyses
删除的内容: ,
删除的内容: i
删除的内容: weighed
删除的内容: by
删除的内容: Moreover, f
删除的内容: eliminate the
删除的内容: analyzed
删除的内容: by
删除的内容: Inc.

were determined using a Desert Research Institute (DRI) Model 2001 thermal/optical carbon analyzer (Atmoslytic Inc., Calabasa, CA, USA) following the Interagency Monitoring of Protected Visual Environments (IMPROVE_A) protocol (Chow et al., 2007). A standard sucrose solution was used to establish a standard carbon curve before the analytical runs. Replicate analyses were performed at a rate of one sample for every ten samples, and the repeatability was found to be < 15% for OC and < 10% for EC. More information of the OC and EC measurement procedures may be found in Cao et al. (2003). Thirteen elements were determined by energy-dispersive X-ray fluorescence (ED-XRF) spectrometry (Epsilon 5 ED-XRF, PANalytical B.V., Netherlands), and these elements include Al, Si, K, Ca, Ti, Cr, Mn, Fe, Cu, Zn, As, Br, and Pb. The analytical accuracy for ED-XRF measurements was determined with a NIST Standard Reference Material 2783 (National Institute of Standards and Technology, Gaithersburg, MD, USA). A more detailed description of the ED-XRF methods may be found in Xu et al. (2012).

2.2.2 Online measurements

The aerosol optical properties were determined using a Photoacoustic Extinctiometer (PAX, Droplet Measurement Technologies, Boulder, CO, USA) at a wavelength of 532 nm. The PAX measured light scattering (b_{scat}) and absorption (b_{abs}) coefficients (in Mm^{-1}) simultaneously using a built-in wide-angle integrating reciprocal nephelometer and an photoaucoustic technique, respectively. Before and during the sampling, the PAX b_{scat} and b_{abs} were calibrated using ammonium sulfate and fullerene soot particles, respectively, which were generated with an atomizer (Model 9302, TSI Inc., Shoreview, MN, USA). Detailed calibration procedures have been described in Wang et al. (2018a; 2018b). For this study, the PAX was fitted with a $PM_{2.5}$ cutoff inlet, and the sampled particles were dried by a Nafion® dryer (MD-700-24S-1; Perma Pure, LLC., Lakewood, NJ, USA). The time resolution of the data logger was set to 1 minute.

One-minute average mixing ratios of NOx (NO + NO_2), O_3, and SO_2 were measured using a Model 42*i* gas-phase chemiluminescence NOx analyzer (Thermo Fisher Scientific, Inc., Waltham, MA, USA), a Model 49*i* photometric ozone analyzer (Thermo Fisher Scientific, Inc.), and a Model 43*i* pulsed UV fluorescence analyzer (Thermo Fisher Scientific, Inc.), respectively. Standard reference NO, O_3, and SO_2 gases were used to calibrate the NOx, O_3, and SO_2 analyzers, respectively, before and during the campaign. All the online data were averaged to 24 h and matched to the duration of the filter sampling.

删除的内容: Different concentration gradients of
删除的内容: were
删除的内容: analysis
删除的内容: Moreover, r
删除的内容: in
删除的内容: is
删除的内容: better than
删除的内容: in this study
删除的内容: s
删除的内容: an
删除的内容: d
删除的内容: M
删除的内容: measures
删除的内容: of
删除的内容: the PAX
删除的内容: with a set of different concentration gradients of
删除的内容: is
删除的内容: In
删除的内容: inlet of
删除的内容: installed
删除的内容: according

2.2.3 Complementary data

Wind speed (WS) and relative humidity (RH) were measured with the use of an automatic weather station installed at the Xianghe Atmospheric Observatory. Surface weather charts for East Asia were obtained from the Korea Meteorological Administration. The three-day backward in time trajectories and mixed layer heights (MLHs) were calculated using the Hybrid Single-Particle Lagrangian Integrated Trajectory (HYSPLIT) model (Draxler and Rolph, 2003), which was developed by the National Oceanic and Atmospheric Administration (NOAA). The aerosol optical depth (AOD) was measured using a sunphotometer (Cimel Electronique, Paris, France), and those data were obtained from the Aerosol Robotic Network data archive (http://aeronet.gsfc.nasa.gov). Fire counts were obtained from the Moderate Resolution Imaging Spectroradiometer (MODIS) instruments on the Aqua and Terra satellites (https://firms.modaps.eosdis.nasa.gov/map).

2.3 Data analysis methods

2.3.1 Chemical mass closure

The chemically reconstructed $PM_{2.5}$ mass was calculated as the sum of OM, EC, SO_4^{2-}, NO_3^-, NH_4^+, Cl^-, fine soil, and trace elements. A factor of 1.6 was used to convert OC to OM (OM = 1.6 × OC) to account for those unmeasured atoms in organic materials based on the results of Xu et al. (2015). The mass concentration of fine soil was calculated by summing the masses of Al, Si, K, Ca, Ti, Mn, and Fe oxides using the following equation (Cheung et al., 2011):

$$[\text{Fine soil}] = [Al_2O_3] + [SiO_2] + [K_2O] + [CaO] + [TiO_2] + [MnO_2] + [Fe_2O_3] = 1.89 \times [Al] + 2.14 \times [Si] + 1.21 \times [K] + 1.4 \times [Ca] + 1.67 \times [Ti] + 1.58 \times [Mn] + 1.43 \times [Fe] \quad (1)$$

The mass concentration of trace elements was calculated as the sum of measured elements that were not used in the calculation of fine soil:

$$[\text{Trace elements}] = [Cr] + [Cu] + [Zn] + [As] + [Br] + [Pb] \quad (2)$$

As shown in Figure S1, the reconstructed $PM_{2.5}$ mass was strongly correlated (r = 0.98) with the gravimetrically determined values, and this attests to the validity of the chemical reconstruction method. The slope of 0.86 indicates that our measured chemical species accounted for most of the $PM_{2.5}$ mass. The difference between the reconstructed and measured $PM_{2.5}$ mass was defined as "others".

删除的内容: The
删除的内容: at the surface
删除的内容: accessible
删除的内容: derived
删除的内容: from
删除的内容: is
删除的内容: these
删除的内容: can be
删除的内容: freely
删除的内容: The f
删除的内容: observations
删除的内容: Based on the results of Xu et al. (2015), a
删除的内容: adopted
删除的内容: , and the
删除的内容: is as follows
删除的内容:
删除的内容:
删除的内容: estimated
删除的内容: the
删除的内容: did
删除的内容: be
删除的内容:
删除的内容: is
删除的内容: value from
删除的内容: measurement
删除的内容: suggesting strong reliability
删除的内容: discrepancy

2.3.2 Receptor model source apportionment

Positive matrix factorization (PMF) has been widely used in source apportionment studies in the past two decades (e.g., Cao et al., 2012; Xiao et al., 2014; Tao et al., 2014; Huang et al., 2017). The principles of PMF are described in detail elsewhere (Paatero and Tapper, 2006). Briefly, PMF is a bilinear factor model that decomposes an initial chemically-speciated dataset into a factor contribution matrix G_{ik} ($i \times k$ dimensions) and a factor profiles matrix F_{kj} ($k \times j$ dimensions), and then iteratively minimizes the object function Q:

$$X_{ij} = \sum_{k=1}^{p} G_{ik} F_{kj} + E_{ij} \quad (3)$$

$$Q = \sum_{i=1}^{m} \sum_{j=1}^{n} \left(\frac{E_{ij}}{\sigma_{ij}}\right)^2 \quad (4)$$

where X_{ij} is the concentration of the jth species measured in the ith sample; E_{ij} is the model residual; and σ_{ij} represents the uncertainty.

In this study, the PMF Model version 5.0 (PMF 5.0) from US Environmental Protection Agency (EPA) (Norris et al., 2014) was employed to identify the $PM_{2.5}$ sources. Four to nine factors were extracted to determine the optimal number of factors with random starting points. When the values of scaled residuals for all chemical species varied between -3 and +3 and a small Q_{true}/Q_{expect} was obtained, the base run was considered to be stable. Further, bootstrap analysis (BS), displacement analysis (DISP), and bootstrap-displacement analysis (BS-DISP) were applied to assess the variability and stability of the results. A more detailed description of the methods for the determination of uncertainties in PMF solutions can be found in Norris et al. (2014).

2.3.3 Regional chemical dynamical model

The Weather Research and Forecasting model coupled to chemistry model (WRF-Chem) is a 3-D online-coupled meteorology and chemistry model, and it was used to simulate the formation processes that led to high $PM_{2.5}$ loadings after the NCCPC. The WRF-Chem uses meteorological information, including clouds, boundary layer, temperature, and winds; pollutant emissions; chemical transformation; transport (e.g., advection, convective, and diffusive); photolysis and radiation; dry and wet deposition; and aerosol interactions. A detailed description of the WRF-Chem model may be found in Li et al. (2011a; 2011b; 2012). A grid of 280 × 160 cells covering China with a horizontal resolution of 0.25° was used for the simulation, which also included twenty-eight vertical layers from the Earth's surface up to 50 hPa. Seven layers below 1 km were used to ensure a high vertical resolution near ground-level. The meteorological

删除的内容: chemically …hemically-speciated dataset into a factor contributions ... [10]

删除的内容:

删除的内容:

删除的内容: that …easured in the *i*th sample; E_{ij} is the model residuals ... [11]

删除的内容: source factors that contributed to …$M_{2.5}$ sourcesmass… Four to nine factors were extracted to determine the optimal number of factors with random starting points. When the values of scaled residuals for all chemical species vary …aried between -3 and +3 and a small Q_{true}/Q_{expect} is …as obtained, the base run was could be …onsidered as …o be stable. Further, the …ootstrap analysis (BS), displacement analysis (DISP), and bootstrap-displacement analysis (BS-DISP) were applied to assess the variability and stability of the results. A More …ore detailed description of the determination …ethods of …or the determination of uncertainties for ... [12]

删除的内容: (Weather Research and Forecasting model coupled to chemistry) …s a 3-D online-coupled meteorology and chemistry model, and it is …as used to simulate the formation processes that led toof…high $PM_{2.5}$ loadings in the BTH region during pollution episodes …fter the NCCPC. The WRF-Chem usesincludes the components of…meteorological information, includingprocesses (e.g.,…clouds, boundary layer, temperature, and winds;),…pollutant emissions, … chemical transformation, … transport (e.g., advection, convective, and diffusive), …; photolysis and radiation, … dry and wet deposition, … and aerosol interactions. A Detailed …etailed description of the WRF-Chem model may be found in Li et al. (2011a; 2011b; 2012). A Grid …rid cells …f 280 × 160 cells covering China with a horizontal resolution of 0.25° were …as used for the simulated…imulation, which also included.…tT…enty-eight vertical layers were set …rom the Earth's surface up to 50 hPa, and… Ss…ven layers < …elow 1 km were used established …o ensure a high near-ground ... [13]

initial and boundary conditions were retrieved from the National Centers for Environmental Prediction (NCEP) reanalysis dataset, and the chemical initial and boundary conditions were obtained from the 6 h output of the Model for Ozone and Related chemical Tracers (MOZART, Emmons et al., 2010). In this study, the mean bias (MB), root mean square error (RMSE), and index of agreement (IOA) were used to evaluate the performance of WRF-Chem simulation. The IOA is representative of the relative difference between the predicted and measured values, and it varies from 0 to 1, with 1 indicating perfect performance of the model prediction. These parameters were calculated using the following equations (Li et al., 2011a):

$$MB = \frac{1}{N}\sum_{i=1}^{N}(P_i - O_i) \quad (5)$$

$$RMSE = [\frac{1}{N}\sum_{i=1}^{N}(P_i - O_i)^2]^{\frac{1}{2}} \quad (6)$$

$$IOA = 1 - \frac{\sum_{i=1}^{N}(P_i - O_i)^2}{\sum_{i=1}^{N}(|P_i - P_{ave}| + |O_i - O_{ave}|)^2} \quad (7)$$

where P_i and P_{ave} represent each predicted $PM_{2.5}$ mass concentration and the average value, respectively; O_i and O_{ave} are the observed $PM_{2.5}$ mass concentrations and the average value, respectively; and N is representative of the total number of predictions used for comparison.

2.3.4 Calculations of chemical b_{scat} and b_{abs}

To determine the contributions of individual $PM_{2.5}$ chemical species to particles' optical properties, b_{scat} and b_{abs} were reconstructed based on the major chemical composition of the $PM_{2.5}$ using the revised IMPROVE equations as follows (Pitchford et al., 2007):

$$b_{scat} \approx 2.2 \times f_S(RH) \times [(NH_4)_2SO_4]_{Small} + 4.8 \times f_L(RH) \times [(NH_4)_2SO_4]_{Large} + 2.4 \times f_S(RH) \times [NH_4NO_3]_{Small} + 5.1 \times f_L(RH) \times [NH_4NO_3]_{Large} + 2.8 \times [OM]_{Small} + 6.1 \times [OM]_{Large} + 1 \times [Fine\ soil] \quad (8)$$

$$[X]_{Large} = \frac{[X]^2}{20\ \mu g\ m^{-3}}, for\ [X] < 20\ \mu g\ m^{-3} \quad (9)$$

$$[X]_{Large} = [X], for\ [X] \geq 20\ \mu g\ m^{-3} \quad (10)$$

$$[X]_{Small} = [X] - [X]_{Large} \quad (11)$$

where the mass concentrations of ammonium sulfate ($[(NH_4)_2SO_4]$) and ammonium nitrate ($[NH_4NO_3]$) were estimated by multiplying the concentrations of SO_4^{2-} and NO_3^- by factors of 1.375 and 1.29,

删除的内容: MOZART
删除的内容: Model for Ozone and Related chemical Tracers) (
删除的内容: are
删除的内容:
删除的内容:
删除的内容:
删除的内容: ir
删除的内容: s
删除的内容: each
删除的内容: ir
删除的内容: s
删除的内容: the
删除的内容: the
删除的内容: in
删除的内容: a

781 respectively (Tao et al., 2014); f(RH) is the water growth for the small (S) and large (L) modes of
782 $(NH_4)_2SO_4$ and NH_4NO_3 in $PM_{2.5}$; and [X] represents the $PM_{2.5}$ composition as used in Eq. (8). This
783 analysis is based on the assumption that the particles were externally mixed. More detailed information
784 of the IMPROVE algorithms may be found in Pitchford et al. (2007).
785 A second assumption for this part of the study was that there was negligible absorption by brown carbon
786 in the visible region (Yang et al., 2009), and on this basis, the b_{abs} can be determined from the EC mass
787 concentration using linear regression (Eq. 12). As shown in Figure S2, the derived slope (a) and intercept
788 (b) for the regression model were 10.8 m^2 g^{-1} and -4.7, respectively.

789 $$b_{\text{abs}} = \text{a} \times [\text{EC}] + \text{b} \quad (12)$$

790 **2.3.5 DRF calculation**

791 The Tropospheric Ultraviolet and Visible (TUV) radiation model developed by the National Center for
792 Atmospheric Research was used to estimate the aerosol DRF for 180 – 730 nm at the Earth's surface. A
793 detailed description of the model may be found in Madronich (1993). Aerosol DRF is mainly controlled
794 by the aerosol column burden and chemical composition, and important properties include the AOD,
795 aerosol absorption optical depth (AAOD), and single-scattering albedo (SSA = (AOD-AAOD)/AOD).
796 Based on an established relationship between the AODs measured with sunphotometer and the light
797 extinction coefficients ($b_{ext} = b_{scat} + b_{abs}$) observed with PAX, an effective height can be retrieved which
798 makes it possible to convert the IMPROVE-based chemical b_{ext} values into the AODs or AAODs caused
799 by the $PM_{2.5}$. There are hygroscopic effects to consider, and therefore, the dry b_{ext} values measured here
800 were modified to the wet b_{ext} based on the water-growth function of particles described in Malm et al.
801 (2003). We note that the estimated chemical AODs were based on the assumption that the aerosols were
802 distributed homogeneously throughout an effective height.
803 Finally, the calculated chemical AOD and SSA for different $PM_{2.5}$ composition scenarios were used in
804 the TUV model to obtain shortwave radiative fluxes. Values for the surface albedo, another factor that
805 influences DRF, were obtained from the MOD43B3 product measured with the Moderate Resolution
806 Imaging Spectroradiometer (https://modis-atmos.gsfc.nasa.gov/ALBEDO/index.html). The solar
807 component in the TUV model was calculated using the δ-Eddington approximation, and the vertical
808 profile of b_{ext} used in the model was described in Palancar and Toselli (2004). The aerosol DRF is defined
809 as the difference between the net shortwave radiative flux with and without aerosol as follows:

810 $$DRF_{surface} = Flux\ (net)_{with\ aerosol,\ surface} - Flux\ (net)_{without\ aerosol,\ surface} \quad (13)$$

删除的内容: involved…in Eq. (8). This analysis is based on the premise …ssumption that theof…particles were being …xternally mixed. More detailed information of the IMPROVE algorithms is …ay be founddescribed ... [14]

删除的内容: Considering that EC is the dominant species absorbing light in the visible region (e.g., 532 nm) (Massabò et al., 2015), the relationship between …abs can be determined from theand…EC mass concentration is …sing linear regression (Eq. 12). As shown in Figure S2, the derived slope (a) and intercept (b) for thedetermined by a linear…regression model were 10.8 m^2 g^{-1} and -4.7, respectively.: ... [15]

删除的内容: (NCAR) is…as used to estimate the aerosol DRF for 180 – 730 nm at the Earth's surface. A detailed description of the model may be found in Madronich (1993). Aerosol DRF is mainly controlledaffected…by the aerosol column burden and its…chemical composition, and important properties include which can be reflected by …he parameters of …OD, aerosol absorption optical depth (AAOD), and single-scattering albedo (SSA = (AOD-AAOD)/AOD). Based on the …n established relationship between the AODs measured with the…sunphotometer and the light extinction coefficients ($b_{ext} = b_{scat} + b_{abs}$) observed with the…PAX, an effective height can be retrieved which makes it possible to convert the IMPROVE-based chemical b_{ext} values into the AODs or AAODs that…caused by the the chemical species in …$M_{2.5}$. There are Due to the influences of …ygroscopic effects to consider, and thereforeproperties of $PM_{2.5}$… the measured …ry b_{ext} values measured here were modified to the wet b_{ext} based on the water …ater-growth function of particles described in Malm William …t al. (2003). We note It should be noted …hat the estimated chemical AOD value… are …ere based on the assumption that the aerosols were are …istributed homogeneously throughout anwithin a given ... [16]

删除的内容: caused by…or different $PM_{2.5}$ composition scenarios were used in the TUV model to obtain the…shortwave radiative fluxes. Values for tT…e surface albedo, another factor that influencesinfluential factor for estimation of…DRF, was …ere obtained from the MOD43B3 product measured with the Moderate Resolution Imaging Spectroradiometer (https://modis-atmos.gsfc.nasa.gov/ALBEDO/index.html). The solar component in the TUV model was calculated usingin view of…the δ-Eddington approximation, and the vertical profile of b_{ext} used in the model is ... [17]

删除的内容: … ... [18]

3 Results and discussion

3.1 Effectiveness of the control measures on reducing $PM_{2.5}$

We divided the study period into two phases based on the dates that the pollution control measures were put into effect (1) the NCCPC-control period from 12 to 24 October and (2) non-control period from 25 October to 4 November. Temporal variations in the $PM_{2.5}$ mass concentrations and those of the major aerosol components during these two phases are shown in Figure 2, and a statistical summary of those data is presented in Table 1. During the NCCPC-control period, the $PM_{2.5}$ mass concentrations remained consistently low relative to the NAAQS II (75 μg m^{-3}), generally < 75 μg m^{-3}. In contrast, higher fine particle loadings ($PM_{2.5}$ > 75 μg m^{-3}) frequently were observed during the non-control period. On average, the mass concentration of $PM_{2.5}$ during the NCCPC-control period was 57.9 ± 9.8 μg m^{-3}, which is lower by 31.2% compared with the non-control period (84.1 ± 38.8 μg m^{-3}). Meanwhile, the $PM_{2.5}$ mass concentrations obtained from the China Environmental Monitoring Center also showed a decreasing trend over most of the BTH region during the NCCPC-control period (see Figure S3). Compared with previous events when pollution control measures were implemented in Beijing and surrounding areas, the percent decrease in $PM_{2.5}$ found for the present study falls within the lower limit of the 30–50% reduction for Olympic Games (Wang et al., 2009; Li et al., 2013), but it is less than the range of 40–60% for the APEC (Tang et al., 2015; Tao et al., 2016; J. Wang et al., 2017) or the range of 60–70% for the VDP (Han et al., 2016; Liang et al., 2017; Lin et al., 2017).

As shown in Figure 2 (right panel), the chemical mass closure calculations for $PM_{2.5}$ showed that on average OM was the largest contributor (30.4%) to $PM_{2.5}$ mass during the non-control period, followed by NO_3^- (16.7%), fine soil (11.2%), and EC (7.6%). In contrast, OM (24.3%) and NO_3^- (22.9%) dominated the $PM_{2.5}$ mass during the NCCPC-control period, followed by SO_4^{2-} (9.8%), NH_4^+ (9.1%), and EC (7.9%). The OM mass concentration was decreased largely by 43.1% from 24.6 μg m^{-3} during the non-control period to 14.0 μg m^{-3} during the NCCPC-control period. For secondary water-soluble inorganic ions, the average mass concentrations of NO_3^- (13.4 μg m^{-3} versus 16.9 μg m^{-3}) and NH_4^+ (5.4 versus 6.8 μg m^{-3}) were lower by 20.7% and 20.6% during the NCCPC-control period, respectively. However, SO_4^{2-} exhibited similar loadings during the NCCPC-control (5.8 μg m^{-3}) and non-control (5.3 μg m^{-3}) periods. This is consistent with the small differences in SO_2 concentrations for the NCCPC-control (8.5 μg m^{-3}, Figure S4) versus the non-control (12.4 μg m^{-3}, Figure S4) periods. Indeed, the low SO_2 concentrations may not have provided sufficient gaseous precursor to form substantial amounts of sulfate. The loadings of EC, Cl^-, and fine soil were lower by 25.0, 44.8, and 40.8%, respectively, when the controls were in

删除的内容: Based on the dates of emission control measures, w…e divided the whole …tudy period into two phases based on the dates that the pollution control measures were put into effect (1):…the NCCPC …CCPC-control period from 12 to 24 October and (2) non-control period from 25 October to 4 November. Temporal variations of …n the $PM_{2.5}$ mass concentrations of $PM_{2.5}$ …nd those of the its…major aerosol components during these two phases are shown in Figure 2, and a statistical summary of those data is presented in Table 1. During the NCCPC-control period, tT…e $PM_{2.5}$ mass concentrations of $PM_{2.5}$ …emained consistently low relative to the NAAQS II (75 μg m^{-3}), generally < 75 μg m^{-3} (NAAQS II) during the NCCPC control period…,…In contrast,but the…higher fine particle loadings with …$PM_{2.5}$ > 75 μg m^{-3}) are…frequently were observed during the non-control period. On average, the mass concentration of $PM_{2.5}$ during the NCCPC …CCPC-control period is …as 57.9 ± 9.8 μg m^{-3}, which is lowerdecreased ... [19]

带格式的: 下标

删除的内容: the …revious important …vents that …henimplemented…pollution control measures were implemented in Beijing and its …urrounding areas, the percent decrease reduction ratio of…n $PM_{2.5}$ in …ound for the present study falls within the lower limit reducing range …f the 30–50% reduction for the…Olympic Games (Wang et al., 2009; Li et al., 2013), but it is lower …ess than the range of 40–60% for the APEC period…(Tang et al., 2015; Tao et al., 2016; J. Wang et al., 2017) and …r the range of 60–70% for the VDP period ... [20]

删除的内容: of …or $PM_{2.5}$ showedreveals…that on average OM is …as the largest contributor (30.4%) to $PM_{2.5}$ mass during the non-control period, followed by NO_3^- (16.7%), fine soil (11.2%), and EC (7.6%). In contrast, OM (24.3%) and NO_3^- (22.9%) both …ominated the $PM_{2.5}$ mass during the NCCPC …CCPC-control period, followed by SO_4^{2-} (9.8%), NH_4^+ (9.1%), and EC (7.9%). The OM mass concentration of OM is…as decreased largely by 43.1% from 24.6 μg m^{-3} during the non-control period to 14.0 μg m^{-3} during the NCCPC …CCPC-control period. For the …econdary water-soluble inorganic ions, the average mass concentrations of NO_3^- (13.4 μg m^{-3} versus 16.9 μg m^{-3}) and NH_4^+ (5.4 versus 6.8 μg m^{-3}) were lowerdecrease…by 20.7% and 20.6% during the NCCPC …CCPC-control period compared with the non-control period… respectively ... [21]

带格式的 ... [22]

删除的内容: may be attributed to…the low SO_2 concentrations (10.3 ± 3.5 μg m^{-3}, Figure S2) during the entire campaign, which …ay not have provided sufficient enough…gaseous precursor to form substantial amounts of sulfate. Furthermore, t…he loadings of EC, Cl^-, and fine soil are …ere reduced …ower by 25.0, 44.8, and 40.8%, respectively, when during …he NCCPC ... [23]

place. The variations in reductions for specific aerosol components imply differences in the effectiveness of the emission controls on the chemical species, but as discussed below, meteorological conditions probably had an influence on the loadings, too.

As shown in Figure S4, both WSs (0.7 ± 0.3 versus 1.3 ± 0.8 m s^{-1}) and MLHs (304.3 ± 60.6 versus 373.7 ± 217.9 m) were lower for the NCCPC-control period compared with the non-control period. This indicates that horizontal and vertical dispersion were weaker during the NCCPC-control period than in the non-control period. More to the point, this shows that one needs to consider the effects of WS and MLH to fully evaluate the effectiveness of the pollution control measures. A simple and effective way to do this is to compare the concentrations of air pollutants for the two periods when atmospheric conditions were stable (Wang et al., 2015; Liang et al., 2017).

We first evaluated atmospheric stability based on relationships between $PM_{2.5}$ mass concentrations and WS and MLH. As shown in Figure 3, the $PM_{2.5}$ mass concentrations exhibited a power function relationship with WS (r = -0.65) and MLH (r = 0.77). The approach used to determine stable conditions was to find the WS and MLH values that were less than the inflection points in the $PM_{2.5}$ loadings; that is, where the slopes in the loadings changed from large to relatively small values. As there are no true inflection points for the power functions, we used piecewise functions to represent them. As shown in Figure 3, the intersections of two linear regressions can be used to represent the inflection points of the influences of meteorological conditions on $PM_{2.5}$ mass. Using these criteria, days with WS < 0.4 m s^{-1} and MLH < 274 m were subjectively considered to have stable atmospheric conditions.

There were two days for the NCCPC-control period and three days for the non-control period that satisfy the stability criteria. The surface charts (Figure S5) show that the weather conditions for those selected stable atmosphere days during the NCCPC-control and non-control periods were mainly controlled by uniform pressure fields and weak low-pressure systems, respectively, and those conditions led to weak or calm surface winds. Due to the lower WS (0.2 versus 0.3 m s^{-1}) and MLH (213 versus 244 m) during the NCCPC-control period relative to the non-control period, the horizontal and vertical dispersion for the stable atmospheric days were slightly weaker during the NCCPC-control period. As shown in Table 1, the percent differences for $PM_{2.5}$ (43.4%), NO_3^- (25.9%), OM (68.1%), EC (40.0%), and fine soil (58.7%) were larger for the days with stable atmospheric conditions compared with those for all days. These results are a further indication that the control measures were effective in reducing pollution, but meteorology also influenced the aerosol pollution.

删除的内容： period compared with the non-control period, respectively… The variations indifferent…reductions for specific aerosol components imply differences in the effectiveness ofeach chemical species revealed their distinct responses to…the emission controls on the chemical species, but as discussed below,and ... [24]

删除的内容: S2…4, both WSs (0.7 ± 0.3 versus 1.3 ± 0.8 m s^{-1}) and MLHs (304.3 ± 60.6 versus 373.7 ± 217.9 m) are…ere lower for the NCCPC …CCPC-control period compared withthan…the non-control period. This indicates that horizontal and vertical diffusion …ispersion were weakerconditions…during the NCCPC …CCPC-control period should be worse …han in the non-control period. More to the point, this shows that one needs Therefore, it is necessary …o consider the effects of WS and MLH to fullywhen further…evaluates…the effectiveness of the pollution control measures. A simple and effective way to do this is to compare the concentrations of air pollutants for the two periods whenunder stable ... [25]

删除的内容: In this study, w…e first evaluated atmospheric stability defined the stable atmospheric conditions…based on the…correlations …elationships between $PM_{2.5}$ mass concentrations and WS and MLH. As shown in Figure 3, the $PM_{2.5}$ mass concentrations exhibits …xhibited a power function relationship with WS (r = -0.65) and MLH (r = 0.77). The approach used to determine criterion for judging …table conditions is …as to findwhether…the WS and MLH values that wereare…lower …ess than the values of turning…nflection points in the $PM_{2.5}$ loadings; that is, where, which are…the slopes in the loadings changed from large to relatively small values. As However, …here is …re no true inflection points for the power functions, thus, …e used piecewise functions to determine the turning points…epresent them. As shown in Figure 3, the intersections of two linear regressions can be representative …sed to represent the inflectionof turning…points of the influences of meteorological conditions on $PM_{2.5}$ mass. Using these criteriaFinally… the…days with WS < 0.4 m s^{-1} and MLH < 274 m are ... [26]

删除的内容: are …ere two days for the NCCPC …CCPC-control period and three days for the non-control period that satisfy the stability criteria criterion… The surface charts (Figure S5) show that the weather conditions for those selected stable atmosphere days during the NCCPC-control and non-control periods were mainly controlled by uniform pressure fields and weak low-pressure systems, respectively, and those conditions led to weak or calm surface winds. Due to the lower WS (0.2 versus 0.3 m s^{-1}) and MLH (213 versus 244 m) during the NCCPC-control period relative to the non-control period, the horizontal and vertical dispersion for the stable atmospheric days were slightly weaker during the NCCPC-control ... [27]

3.2 Estimates of source contributions

The mass concentrations of water-soluble inorganic ions (SO_4^{2-}, NO_3^-, NH_4^+, K^+, and Cl^-), carbonaceous (OC and EC), and elements (Al, Si, Ca, Ti, Cr, Mn, Fe, Cu, Zn, As, Br, and Pb) were used as data inputs for the PMF 5.0 model. Through comparisons between the PMF profiles and reference profiles from previous studies, the presumptive sources for the aerosol were identified as (i) coal combustion, (ii) traffic-related emissions, (iii) secondary particle formation, (iv) biomass burning, (v) industrial processes, and (vi) mineral dust. As shown in Figure S6, the PMF modelled $PM_{2.5}$ mass concentrations were strongly correlated with the observed values (r = 0.98, slope = 0.94), and the model-calculated concentrations for each chemical species exhibited good linearity and correlations with the measured values (r = 0.68–0.99) (Table S1). These results show that the six identified sources were physically interpretable and accounted for much of the variability in the data.

Figure 4 presents the source profiles and the average contribution of each source to $PM_{2.5}$ mass during the NCCPC-control and non-control periods. The first source factor was identified as coal burning emissions because it was enriched with As (38.8%), Pb (32.9%), and Fe (30.3%) and had moderate loadings of Mn (26.2%), Zn (23.8%), Si (23.1%), and Ca (22.8%) (Figure 4a). Of these elements, As is a well-known tracer for coal burning (Hsu et al., 2009; Y. Chen et al., 2017); Pb, Fe, Mn, and Zn (Xu et al., 2012; Men et al., 2018) are enriched in particles generated by this source; and Ca and Si can be components of coal fly ash (Pipal et al., 2011). There was no significant difference in $PM_{2.5}$ loadings contributed by this source between the NCCPC-control (8.5 μg m^{-3}) and non-control (7.8 μg m^{-3}) periods. This may be because coal burning is mainly used for domestic purposes, especially heating, and the control measures did not include this sector. The contribution of coal burning to $PM_{2.5}$ mass in our October/November study was lower than its contribution in the BTH region in winter (~20 – 60 μg m^{-3}) (Huang et al., 2017), and that can be explained by the increased domestic usage of coal for heating activities during the colder winter season.

The second source factor was linked to traffic-related emissions, and it was characterized by strong loadings of EC (42.1%) and Cu (40.7%) and moderate contributions of OC (29.1%), Zn (27.1%), and Br (22.2%). Previous studies have indicated that carbonaceous aerosols are components of gasoline and diesel engine exhaust (Cao et al., 2005), and therefore, EC and OC have been used as indicators for motor vehicle emissions (Chalbot et al., 2013; Khan et al., 2016a), and Br, too, may be emitted from internal combustion engines (Bukowiecki et al., 2005). Aerosol Cu and Zn are derived from other types of vehicle emissions, including those associated with lubricant and oil, brake linings, metal brake wear, and tires

删除的内容: **ion**

删除的内容: inputs… Through comparisons After compared…etween the PMF profiles andwith the…reference profiles from previous literatures…tudies, the finally identified…resumptive sources for the aerosol were identified asare…(i) coal combustion, (ii) traffic-related emissions, (iii) secondary inorganic aerosols…article formation, (iv) biomass burning, (v) industrial processes, and (vi) mineral dust. As shown in Figure S3…6, the PMF modelled $PM_{2.5}$ mass concentrations are …ere strongly correlated with the observed values (r = 0.98,) with a…slope =of…0.94), and simultaneously, …he model-calculated concentrations of …or each modelled …hemical species represent …xhibited goodness-of-fit of…linearity and correlations regression…with the measured values (r = 0.68–0.99) (Table S1). These results reveal…how that the six identified sources could be…ere reasonably …hysically interpretable and accounted for much of the variability in the dataprofiles in this study ... [28]

删除的内容: NCCPC …CCPC-control and non-control periods. As shown in Figure 4a, t…he first source factor is …as identified as coal burning emissions because it was enriched in …ith As (38.8%), Pb (32.9%), and Fe (30.3%) as well as…nd had moderate contributions from…oadings of Mn (26.2%), Zn (23.8%), Si (23.1%), and Ca (22.8%) (Figure 4a). Of these elements,The…As has …s a well-known been proposed as a useful …racer for coal burning (Hsu et al., 2009; Y. Chen et al., 2017). …; Moreover, the metals of ... [29]

已移动(插入) [2]

删除的内容: could be produced from the processes of coal combustion (Xu et al., 2012; Men et al., 2018), while

已上移 [2]: (Xu et al., 2012; Men et al., 2018)

删除的内容: consisted in…omponents of coal fly ash (Pipal et al., 2011). Thus, this source factor is assigned to the coal burning. …here is…as no significant difference in $PM_{2.5}$ mass …oadings contributed by this source from coal burning …etween the NCCPC …CCPC-control (8.5 μg m^{-3}) and non-control (7.8 μg m^{-3}) periods. This may be due to the fact that…ecause coal burning is mainly used for household energy for local residents…omestic purposes, especially heating, and whereas…the control measures do …id not involve …nclude this sector. The contribution of coal burning to $PM_{2.5}$ mass in our October/November study wasfrom this source is…lower than the …ts contribution values (~20 – 60 μg m^{-3}) from ... [30]

删除的内容: is…as linked to traffic-related emissions, and it was …haracterized by the elevated…trong loadings of EC (42.1%) and Cu (40.7%) as well as…nd moderate contributions of OC (29.1%), Zn (27.1%), and Br (22.2%). Previous studies have indicated that carbonaceous aerosols are components of strongly ... [31]

(Lin et al., 2015). Furthermore, the mass concentration of $PM_{2.5}$ from this source was strongly correlated ($r = 0.72$) with vehicle-related NOx concentrations (Figure S7), which further suggests the validity of this PMF-resolved source. Traffic-related emissions showed similar percent contributions to $PM_{2.5}$ mass during the NCCPC-control (14.8%) and non-control (15.4%) periods (Figure 4c), but the mass concentration was 38% lower for the NCCPC-control period (8.9 μg m^{-3}) than the non-control period (14.4 μg m^{-3}). This shows that the reduction in motor vehicle activity during the control period led to better air quality.

The third source factor was a clear signal of secondary particle formation because it was dominated by high loadings of SO_4^{2-} (45.4%), NO_3^- (43.4%), and NH_4^+ (47.0%) (Zhang et al., 2013; Amil et al., 2016). Moreover, moderate loadings of As (30.5%), Pb (27.4%), Cr (31.4%), Cu (30.7%), and EC (30.8%) also were assigned to this factor, suggesting influences from coal burning and vehicle exhaust emissions. Although the concentrations of gaseous precursors, especially SO_2 and NOx, were lower during the NCCPC-control period (Figure S4), the average mass contribution of secondary $PM_{2.5}$ was larger when the controls were in effect (22.5 versus 18.3 μg m^{-3}); indeed, this source was the largest contributing factor (37.3% of $PM_{2.5}$ mass) during the NCCPC-control period. We note that the higher RH (84%) during the NCCPC-control period compared with the non-control period (69%) may have promoted the formation of the secondary inorganic aerosols through aqueous reactions (Sun et al., 2014).

The fourth source factor, identified as emissions from biomass burning, was characterized by the high loadings of K^+ (59.5%) with moderate loadings of Cl^- (33.3%), OC (28.5%), NO_3^- (37.1%), SO_4^{2-} (21.1%), and NH_4^+ (39.6%). Soluble K^+ is an established tracer for biomass burning (Zhang et al., 2013; Wang et al., 2016b), and Cl^- and OC also are emitted during biomass burning (Tao et al., 2014; Huang et al., 2017). Previous studies have shown that SO_2 and NO_2 can be converted into sulfate and nitrate on KCl particles during the transport of biomass-burning emissions (Du et al., 2011). Therefore, the abundant NO_3^-, SO_4^{2-}, and NH_4^+ associated with this factor may be indicative of aged biomass-burning particles. As shown in Figure 4c, biomass burning contributed substantially to $PM_{2.5}$ mass during both the NCCPC (21.6%) and non-control periods (27.3%). This is to be expected because Hebei Province is a major corn and wheat producing area, and the residues of these crops commonly are used for residential cooking and heating or burned in the fields (J. Chen et al., 2017). The mass concentrations of $PM_{2.5}$ from this source were lower during the NCCPC (13.0 μg m^{-3}) than in the non-control period (25.7 μg m^{-3}), and this indicates the effectiveness of the control policy that forbade the open space biomass-burning during the NCCPC. As

删除的内容：Br may be partly emitted from fuel combustion in internal combustion engines (Bukowiecki et al., 2005). Therefore, the second source factor is representative of traffic-related emissions. …urthermore, the mass concentration of $PM_{2.5}$ from this source is …as strongly correlated ($r = 0.72$) with the …ehicle-related NOx concentrations (Figure S4…7), which further suggests the validity of the …his PMF-resolved source contributions… The t…affic-related emissions have …howed similar percentages of…contributions to $PM_{2.5}$ mass during the NCCPC …CCPC-control (14.8%) and non-control (15.4%) periods (Figure 4c), but its …he mass concentration is …as 38%1.6 times…lower for the NCCPC …CCPC-control period (8.9 μg m^{-3}) than the non-control period (14.4 μg m^{-3}). This is attributed to…hows that the reduction of …n motor vehicle activity volume on road by traffic restriction. ... [32]

删除的内容：is …as a clear signal of secondary particle formation because it was dominated by the ... [33]

已移动(插入) [3]

删除的内容：), …. and is obviously classified as secondary inorganic aerosol (Zhang et al., 2013; Amil et al., 2016). ... [34]

已上移 [3]：(Zhang et al., 2013; Amil et al., 2016)

删除的内容：are also…assigned to this factor, suggesting the …nfluences of…rom coal burning and vehicle exhaust emissionss… Although the concentrations of gaseous precursors, especially (e.g.,…SO_2 and NOx,)…were lower during the NCCPC …CCPC-control period are lower than the non-control period…(Figure S42…, the average mass contribution of secondary $PM_{2.5}$ from source of secondary inorganic aerosol is…as larger when during …he NCCPC …ontrols were in effectperiod…(22.5 versus 18.3 μg m^{-3}), …; indeed,and…this source becomes …as the largest contribution …ontributing factor (37.3% of $PM_{2.5}$ mass) during the NCCPC …CCPC-control period. We note that Compared with the low RH (69%) during the non-control period, …he higher RH (84%) during the NCCPC …CCPC-control period compared with the non-control period (69%) may havecould ... [35]

删除的内容：is…characterized by the high contributions …oadings of K^+ (59.5%) with moderate loadings of Cl^- (33.3%), OC (28.5%), NO_3^- (37.1%), SO_4^{2-} (21.1%), and NH_4^+ (39.6%). Soluble K^+ is an establisheda good…tracer for biomass burning (Zhang et al., 2013; Wang et al., 2016b), and Cl^- and OC also are emitted during biomass burning also related to this source …Tao et al., 2014; Huang et al., 2017). Consequently, this factor is assigned to the biomass burning. …revious studies have found …hown that SO_2 and NO_2 can be converted into sulfate and nitrate aerosols …n the surface of pre-existing…KCl particles during the regional …ransport of biomass-burning emissions (Du et al., 2011). Therefore, the abundant NO_3^-, SO_4^{2-}, and NH_4^+ associated with this factor may be indicative of aged ... [36]

the control measures did not include prohibitions on the household use of biofuels, substantial contributions of biomass burning were still evident during the NCCPC-control period.

The fifth source factor was identified as emissions from industrial processes because it had high loadings of Zn (41.3%), Br (38.0%), Pb (19.9%), As (19.2%), Cu (17.5%), and Mn (19.1%) (Q. Q. Wang et al., 2017; Sammaritano et al., 2018). This source contributed 3.6 μg m^{-3} to $PM_{2.5}$ mass during the NCCPC-control period, which is lower than the non-control period (16.2 μg m^{-3}) by 78%, and its percent contribution to $PM_{2.5}$ mass also increased correspondingly from 6.0 to 17.2% after the controls were removed. The results show that restrictions on industrial activities during the NCCPC-control period led to improvements in air quality. Iron and steel production are among the most important industries in BTH region, and the iron and steel production there accounted for 28.8% of the total for China in 2016 (NBS, 2017). The sintering process in iron and steel industries produce large amounts of heavy metal pollutants including Zn, Pb, and Mn (Duan and Tan, 2013). Hence, the iron and steel industries in the BTH region were probable sources for these metals during the non-control period.

The sixth source factor was obviously mineral dust because it had high loadings of Al (55.9%), Si (55.7%), Ca (52.6%), and Ti (36.7%) (Zhang et al., 2013; Tao et al., 2014; Kuang et al., 2015). This factor contributed 3.8 μg m^{-3} (6.3% of $PM_{2.5}$ mass) during the NCCPC-control period and 11.5 μg m^{-3} (12.3%) to $PM_{2.5}$ mass in the non-control period. Possible sources for the mineral dust include (i) natural dust, which contains crustal Al, Si, and Ti (Milando et al., 2016), (ii) construction dust, which includes Ca (Liu et al., 2017), and (iii) road dust, which is characterized by traffic-related species, such as Cu, Zn, Br, and EC (Khan et al., 2016b; Zong et al., 2016). Here, the mineral dust factor did not contain any notable contributions from the traffic-related species. Thus, this factor can be explained by the natural and construction dusts. As shown in Figure S8, WS was positively correlated (r = 0.75) with the $PM_{2.5}$ mass from mineral dust. To reduce the effects of wind speed on crustal dust resuspension, we compared the days with low winds (< 1 m s^{-1}) during the sampling periods, and only three sampling days were excluded from the analysis. This comparison showed that the mass concentration of $PM_{2.5}$ from mineral dust was 60% lower in the NCCPC-control period (3.8 μg m^{-3}) compared with the non-control period (9.5 μg m^{-3}). This is a strong indication that restrictions on construction activities during the NCCPC-period were effective in reducing the mineral dust component of $PM_{2.5}$, but as noted above, this was not a large component of the $PM_{2.5}$ mass.

删除的内容: do …id not involve …nclude prohibitions on the household use of biofuels, substantial and thus, the high …ontributions of biomass burning can be…ere still evidentmeasured…during the NCCPC ... [37]

删除的内容: have…high loadings on …f Zn (41.3%), Br (38.0%), Pb (19.9%), As (19.2%), Cu (17.5%), and Mn (19.1%), and is thought to be associated with industrial process emissions…(Q. Q. Wang et al., 2017; Sammaritano et al., 2018). This source contributes …ontributed 3.6 μg m^{-3} to $PM_{2.5}$ mass during the NCCPC …CCPC-control period, which is lower than the non-control period (16.2 μg m^{-3}) by 78%a factor of 4.5… and its percentage of…contribution to $PM_{2.5}$ mass also increases …ncreased correspondingly from 6.0 to 17.2% accordingly…fter the controls were removed. The results show that reveal the effectiveness of …estrictions on industrial activities during the NCCPC …CCPC-control period led to improvements in air quality. Iron and steel factory …roduction are amongis one of…the most important industries in BTH region, and the scale of …ron and steel production theres…accounteds…for 28.8% of the total amount of…or China in 2016 (NBS, 2017). The sintering process in the…iron and steel industries can…produce large amountsplenty…of heavy metal pollutants including Zn, Pb, and Mn (Duan and Tan, 2013). Hence, the iron and steel industries in the BTH region may be possibly important…ere probable sources for these metals amongst industrial processes ... [38]

删除的内容: predominant species in the …ixth source factor was obviously mineral dust because it had high loadings ofare…Al (55.9%), Si (55.7%), Ca (52.6%), and Ti (36.7%), which is obviously classified as mineral dust…(Zhang et al., 2013; Tao et al., 2014; Kuang et al., 2015). This factor contributes …ontributed 3.8 μg m^{-3} (6.3% of $PM_{2.5}$ mass) during the NCCPC-control period and 11.5 μg m^{-3} (12.3%) to $PM_{2.5}$ mass during the NCCPC control and…n the non-control periods, respectively… The p…ossible sources for causing …he mineral dust may …nclude (i) natural dust, which contains crustal Al, Si, and Ti (Milando et al., 2016), (ii) construction dust, which includes Ca (Liu et al., 2017), and (iii) road dust, which is characterized byrefers to the…traffic-related species, such as Cu, Zn, Br, and EC (Khan et al., 2016b; Zong et al., 2016). Here, the mineral dust factor do …id not contain any notable contributions from the traffic-related species. Thus, this factor can be explained may be mainly influenced …y the natural dust …nd construction activities…usts. As shown in Figure S5…8, WS is …as positively correlated well …r = 0.75) with the $PM_{2.5}$ mass that is contributed by…rom mineral dust. To reduce the effectsimpact…of wind speeds…on crustal dust resuspension, we only …ompared the days with low winds (< 1 m s^{-1}) during the sampling periods, and only ... [39]

3.3 Exploring the pollution episodes after the NCCPC control period

As shown in Figure 2 (left panel), two pollution episodes occurred after the NCCPC-control period (PE1: 25–27 October and PE2: 31 October–1 November); the average $PM_{2.5}$ mass concentrations in PE1 and PE2 were 117.5 and 124.5 μg m^{-3}, respectively. For PE1, secondary aerosols were the dominant contributor to the fine particle population, accounting for 54.6% of $PM_{2.5}$ mass (Figure 5a), and the secondary species that showed the largest contribution to $PM_{2.5}$ mass was NO_3^- (26.8%) (Figure 5b). The mass concentration of NO_3^- increased from ≤ 10 μg m^{-3} before PE1 to ≥ 25 μg m^{-3} during the episode (Figure 2). Molar ratios of NO_3^- to NO_2 (NOR = n-NO_3^-/(n-NO_2 + n-NO_3^-)) were calculated to investigate nitrogen partitioning between the particulate and gas phases (Zhang et al., 2011). As shown in Figure 6a, the mass concentration of $PM_{2.5}$ increased with NOR (r = 0.65) throughout the entire campaign, which indicates that nitrate formation was involved in the high $PM_{2.5}$ loadings. The NORs ranged from 0.32 to 0.71 during the PE1, and those values were significantly different (*t*-test, $p < 0.01$) from the ratios before (0.23–0.29) or after PE1 (0.03–0.10), thus reflecting stronger nitrate formation during the pollution period. Furthermore, NOR exhibited an exponential increase with RH (r = 0.80, Figure 6b), and the higher RHs (91–93%) during the PE1 may have led to greater aqueous nitrate production relative to the periods before (80–86%) or after (33–57%) the first pollution episode.

The second largest contributor to $PM_{2.5}$ mass during PE1 was OM, which accounted for 22.9% of the fine aerosol mass. A widely used EC-tracer method (Lim and Turpin, 2002) was used to estimate the primary and secondary OA (POA and SOA). For this, the lowest 10% percentile of the measured OC/EC ratios was used as a measure of the primary OC/EC ratio (Zheng et al., 2015). The estimated mass concentrations of POA and SOA were 17.2 and 9.7 μg m^{-3} during the PE1, which accounted to 63.9 and 36.1% of the OM mass, respectively.

Photochemical oxidation and aqueous reactions are two of the major mechanisms that lead to the formation SOA (Hallquist et al., 2009), and we evaluated the roles of these chemical reactions by investigating trends in the EC-scaled concentrations of SOA (SOA/EC). We note that normalizing the data in this way eliminates the impacts of different dilution/mixing conditions on the SOA loadings (Zheng et al., 2015). As shown in Figure 6c, the SOA/EC ratios increased (r = 0.65) with Ox (NO_2 + O_3), which is a proxy for atmospheric aging caused by photochemical reactions (Canonaco et al., 2015), and the EC-scaled concentrations showed a weak correlation with RH (r = -0.32) (Figure 6d). These results indicate that photochemical reactions rather than aqueous phase oxidation were the major pathways for

删除的内容：there are …wo pollution episodes occurred after the NCCPC-control period (PE1: 25–27 October and PE2: 31 October–1 November 1… occurred subsequently after the NCCPC control period,… and…the average $PM_{2.5}$ mass concentrations of …n PE1 and PE2 were$PM_{2.5}$ are…117.5 and 124.5 μg m^{-3} on PE1 and PE2… respectively. For PE1, the…secondary inorganic …erosols were is…the dominant contributor to the fine particle populationsource… accounting for 54.6% of $PM_{2.5}$ mass (Figure 5a), and the secondary species that showed of which …he formation of NO_3^- is the most important due to its …argest contribution to $PM_{2.5}$ mass was NO_3^- (26.8%) (Figure 5b). The mass concentration of NO_3^- increases …ncreased from less than… 10 μg m^{-3} before PE1 to greater than… 25 μg m^{-3} during the episodePE1…(Figure 2). Further, we quantified the m…olar ratios of NO_3^- to NO_2 (NOR = n-NO_3^-/(n-NO_2 + n-NO_3^-)) were calculated to investigate, which can be used to reflect…nitrogen partitioning between the particle …articulate and gas phases (Zhang et al., 2011). As shown in Figure 6a, the mass concentration of $PM_{2.5}$ enhances with the …ncreased with NOR (r = 0.65) throughoutduring…the entire campaign, which indicates thatsuggesting…nitrate formation was involvedplays an important role…in accumulation of…he high $PM_{2.5}$ loadings. The NORs ranges …anged from 0.32 to 0.71 during the PE1, and those values werewhich is…significantly different higher…(*t*-test, $p < 0.01$) from the ratios than those …efore (0.23–0.29) or after PE1 (0.03–0.10) … [40]

删除的内容：Furthermore, …M, which is the second largest contributor during the PE1,…accounting …ccounted for 22.9% of the $PM_{2.5}$…ine aerosol mass. The … widely used EC-tracer method (Lim and Turpin, 2002) was applied …sed to estimate the primary and secondary OA (POA and SOA), …. For this,and…the lowest 10% percentile of the measured OC/EC ratios is …as used as a measure ofto identify…the primary OC/EC ratio (Zheng et al., 2015). The estimated mass concentrations of POA and SOA are …ere 17.2 and 9.7 μg m^{-3} during the PE1, which accoun…ccounted toting for … [41]

删除的内容：for …hat lead to the formation SOA formation…(Hallquist et al., 2009). …, and weTo…evaluated the roles of these chemical reactions by investigating trends in,…the EC-scaled concentrations of SOA (SOA/EC). We note that normalizing the data in this way was used to …liminates the impacts of different dilution/mixing conditions on the SOA loadings (Zheng et al., 2015). As shown in Figure 6c, the SOA/EC ratios increaseds…(r = 0.65) with the enhanced …x (NO_2 + O_3), which is a proxy for atmospheric aging caused by photochemical reactions (Canonaco et al., 2015), but it…nd the EC-scaled concentrations showeds…a weak correlation with RH (r = -0.32) (Figure 6d). These results indicate that photochemical reactions rather than aqueous phase oxidation may be…ere the major reaction …athways mechanism … [42]

SOA formation. Thus, the small contribution of SOA to $PM_{2.5}$ during the PE1 may have been due to low photochemical activity during that episode.

In contrast to the first pollution episode, OM (31.8%) was the most abundant $PM_{2.5}$ species during PE2, and that was followed by NO_3^- (19.2%) (Figure 5b). The mass concentration of K^+ increased substantially, from 0.1 μg m^{-3} before PE2 to 1.7 μg m^{-3} during the event, indicating a strengthening influence of biomass-burning emissions. Indeed, the results of PMF show that biomass burning was the largest contributor to $PM_{2.5}$ mass during the PE2, accounting for 36.0% of the total (Figure 5a). Furthermore, the 72-h back trajectories showed that air masses sampled during the PE2 either originated from or passed over areas with fires in Inner Mongolia and Shanxi Province (see Figure 7), and this can explain the apparent impacts from biomass burning emission. Moreover, SOA contributed an estimated 47.7% of the OM mass, and that is a strong indication that secondary organics were a major component of the pollution. The mass concentration of SOA was 19.0 μg m^{-3} during the PE2, and that was higher than in 9.7 μg m^{-3} during the PE1. As the oxidizing conditions—as indicated by Ox—were similar for both pollution episodes (78.0 μg m^{-3} in PE1 versus 86.7 μg m^{-3} in PE2) (Figure S4), the larger SOA during the PE2 can best be explained by SOA that formed from gaseous biomass-burning emissions during transport.

3.4 Meteorological considerations

Previous studies have shown that meteorological conditions play an important role in the accumulation of pollution in the BTH region (Bei et al., 2017). Surface weather charts (Figure 8) were used to analyze the synoptic conditions during the two pollution episodes, and the WRF-Chem model was applied to simulate the formation of $PM_{2.5}$ (Figure 9). As shown in Figure S9, the predicted $PM_{2.5}$ and its major chemical components exhibited trends roughly similar to the observed values. The calculated MB and RMSE for $PM_{2.5}$ were -6.8 and 32.8 μg m^{-3}, and the IOA was 0.75, indicating that the formation of $PM_{2.5}$ during the two pollution episodes was reasonably well captured by the WRF-Chem model even though the predicted average $PM_{2.5}$ mass concentration was lower than the observed value. The most probable reason for this is that uncertainties associated with the complex meteorological fields can affect the transport, diffusion, and removal of air pollutants in the atmosphere (Bei et al., 2012). Additionally, discrepancies in the emission inventories for $PM_{2.5}$ for different years may have contributed to the differences in modelled versus measured values.

On 22 October, that is, before PE1, a weak cold high-pressure system in Siberia moved southward (Figure 8), and the BTH region was under the influence of a cold high-pressure system; conditions such as those tend to keep pollutants at low levels. After the passage of the low-pressure system, the BTH region was

删除的内容： in this study… Thus, the low …mall contribution of SOA to $PM_{2.5}$ during the PE1 may have beenbe…due to the…low photochemical activity under the pollution condition ... [43]

删除的内容：is …as the most abundant $PM_{2.5}$ species in $PM_{2.5}$ …uring the…PE2, and that was followed by NO_3^- (19.2%) (Figure 5b). The mass concentration of K^+ increases …ncreased substantially, from 0.1 μg m^{-3} before the…PE2 to 1.7 μg m^{-3} during the PE2…vent, indicating a strengthening influence of biomass-burning emissions. Indeed, the results of PMF show that biomass burning is …as the largest source …ontributor to $PM_{2.5}$ mass during the PE2, accountingthat accounted…for 36.0% of the total $PM_{2.5}$ mass during the PE2 …Figure 5a). Furthermore, tT…e 72-h backward…trajectory …rajectories analysis …howeds…that a lot of…air masses sampled during the PE2 either originated from or passed over areas withthrough the…fires counts which are located…in the …nner Mongolia and Shanxi Province (see Figure 7), and this can explainindicating…the apparent impacts of …rom transport of …iomass -…urning emissions… Moreover, The estimated …OA contributed an estimateds…47.7% of the OM mass, and that is a strong indication thatreflecting…secondary formation of …rganics were a major component of theplays an important role in aggravating…pollution. The It should be noted that the …ass concentration of SOA was 19.0 μg m^{-3} during the PE2, and that was is…higher than in 9.7 μg m^{-3} during the PE1. AsSince…the oxidizing conditions—as indicated by Ox—were are…similar for both pollution episodes (e.g., Ox: PE1 = …8.0 μg m^{-3} in PE1 versusand…PE2 = …6.7 μg m^{-3} in PE2) (Figure S2…4), the larger ... [44]

删除的内容：indicated …hown that meteorological conditions play an important role in thehave great effects on…accumulation of pollution in the BTH regionpollutants…(Bei et al., 20176.… SurfaceThe…weather charts in …Figure 8) were used to analyze the synoptic conditions during the two pollution episodes, andsystems. Further,…the WRF-Chem model was applied to simulate the formation processes …f $PM_{2.5}$ during the two pollution episodes …Figure 9). As shown in Figure S6…9, the predicted $PM_{2.5}$ and its major chemical composition …omponents exhibited trends roughly similar trends with…o the observed values. The calculated MB and RMSE for $PM_{2.5}$ are …ere -6.8 and 32.8 μg m^{-3}, and the IOA ... [45]

删除的内容：As shown in Figure 8… before PE1, a weak cold high-pressure system in Siberia moved southwardis moving toward south on 22 October…(Figure 8), and the BTH region is …as under the influence ofdominated by…a cold high-pressure system, … conditions such as those tend which is conducive …o keepmaintaining the…pollutants at a …ow levels. After the passage of the low-pressure system,From 24 to 25 October,…the BTH region is ... [46]

under the control of a weak high-pressure system from 24 to 25 October, and that led to a convergence of southernly airflow in the BTH region. Those meteorological conditions were favourable for the gradual accumulation of pollutants (Figure 9). For example, as shown in Figure S4, the NOx concentrations increased from 71.6 μg m^{-3} on 22 October to 147.6 μg m^{-3} on 25 October, and that increase provided a supply of gaseous precursors that can explain the observed large loadings of aerosol nitrate.

On 28 October, the first day of PE1, cold air piled up in the BTH region, and the high-pressure system gradually strengthened. The weather in the BTH region at that time was characterized by cloudiness, high RH, and low surface WSs. Those conditions promoted the accumulation of pollutants (Figure 9), and the WRF-Chem simulation indicated that the BTH region contributed 73.6% of $PM_{2.5}$ mass during PE1. On 29 October, the cold high-pressure system moved towards the south, and northerly winds increased. Those meteorological conditions presumably led to a dilution of the air pollutants, and as a result, lower $PM_{2.5}$ loadings were observed in the BTH region (Figure 9).

From 31 October–1 November (PE2), the BTH region was again dominated by a weak high-pressure system, and a convergence of northerly airflow was caused by the high-pressure system and a trailing low-pressure front. Local pollutants from the BTH region would have accumulated under those conditions, but as discussed above, the loadings of $PM_{2.5}$ also can be affected by the long-range transport processes. Indeed, the WRF-Chem simulation indicated that the BTH region contributed 46.9% to $PM_{2.5}$ mass, similar to the import of fine particles from other regions (53.1%). After 2 November, the cold high-pressure system began to move southward, the winds strengthened, and the air quality gradually improved.

3.5 Impacts of $PM_{2.5}$ emission reduction on aerosol radiative effects

The aerosol DRF refers to the change in the energy balance caused by the scattering and absorption of radiant energy by aerosols. As shown in Figure S10, the reconstructed chemical b_{scat} correlated strongly ($r = 0.91$) with the observed b_{scat} values; the slope of the linear regression was 0.90. This result indicates that the IMPROVE-based method provided a good estimation of the chemical b_{scat}; nonetheless, it is likely that more locally-measured mass scattering efficiencies for each chemical species could reduce the underestimates of measured values. Moreover, a significant ($p < 0.01$) relationship between the measured b_{abs} and EC mass (Figure S2) validates the use of EC mass loadings in Eq. 12 to estimate the chemical b_{abs}. The contributions of each measured $PM_{2.5}$ component to the chemical b_{ext} were calculated based on Eq. 8, and on average, OM was the largest contributor (43.5%) to the chemical b_{ext} during the non-control period (Figure 10a), followed by NH_4NO_3 (32.4%), EC (14.3%), $(NH_4)_2SO_4$ (7.6%), and fine soil (2.2%). In contrast, during the NCCPC-control period, NH_4NO_3 was the largest contributor to the chemical b_{ext},

删除的内容: led by…a weak high-pressure system from 24 to 25 October, and that led followed by a low-pressure system on the rear, and this leads…to a convergence zone …f southernly air …low in the BTH region, … which provides a unfavorable…hose meteorological conditions were favourable for the gradual accumulating …ccumulation of pollutants gradually…(Figure 9). For example, aA… shown in Figure S42… the NOx concentrations increases …ncreased from 71.6 μg m^{-3} on 22 October to 147.6 μg m^{-3} on 25 October, which …nd that increase provides …rovided a supplyhigh level…of gaseous precursors that can explain the observed for formation of…large loadings of aerosol nitrate subsequently ... [47]

删除的内容: During …n 26 – …8 October, the first day of (…E1)… the…cold air is …iled up in the BTH region, and then …he cold…high-pressure system is…gradually strengthened gradually… The weather of …n the BTH region at that time was characterized is dominated …y cloudy…loudiness, high RH, and low surface WSs at this moment… Those unfavourable meteorological …onditions promoted further aggravates …he accumulation of pollutants in this area …Figure 9), and the WRF-Chem simulation indicatedshows…that the BTH region contributes …ontributed 73.6% of $PM_{2.5}$ mass during the…PE1. On 29 October, the cold high-pressure system moves …oved towards the south, and the …ortherly winds increased. Those favourable …eteorological conditions presumably ledlead…to a dilution of the atmospheric ... [48]

删除的内容: During …rom 31 October–1 November (PE2), the BTH region is …as again dominated by a weak high-pressure system, and a convergence of northern…y air …low which is…as caused by the front of weak …igh-pressure system and the … trailingrear of…low-pressure front. The l…ocal pollutants in …rom the BTH region would haveare…accumulated under those weather …onditions, but as discussed above,even though…the loadings of $PM_{2.5}$ also can beare…influenced …ffected by the long-range transport of biomass-burning emissions as we discussed above…rocesses. Indeed, tT…e WRF-Chem simulation indicated reveals …hat the BTH region contributes …ontributed 46.9% to ... [49]

删除的内容: 4

删除的内容: radiative …nergy balance due to…aused by the scattering and absorption of radiant energysunlight…by aerosols. As shown in Figure S7a…10, the reconstructed chemical b_{scat} correlates …orrelated strongly ($r = 0.91$) with the observed b_{scat} values, … thewith a…slope of the linear regression was 0.90, … This result indicates suggesting …hat the IMPROVE-based method provides …rovided a good estimation of the chemical b_{scat}. … nonetheless, it is likely that more locally-measured mass scattering efficiencies for each chemical species could reduce the ... [50]

amounting to 36.7% of b_{ext}, and it was followed by OM (33.3%), EC (16.2%), $(NH_4)_2SO_4$ (11.9%), and fine soil (1.9%). The contributions of the various $PM_{2.5}$ components to b_{ext} were different compared with previous studies of the pollution controls for the Olympics and APEC. For example, Li et al. (2013) reported that $(NH_4)_2SO_4$ (41%) had the largest contribution to b_{ext} during the Olympics, followed by NH_4NO_3 (23%), OM (17%), and EC (9%); Zhou et al. (2017) found that OM (49%) was the largest contributor to b_{ext} during the APEC summit, followed by NH_4NO_3 (19%), $(NH_4)_2SO_4$ (13%), and EC (12%). These differences may be attributed to variable efficiencies of the controls for the specific fine particle species and to variations in RH among studies, the latter of which can influence sulfate and nitrate formation.

As shown in Figure S11, the AODs measured with a sunphotometer were well correlated with the b_{ext} under ambient conditions; the slope (effective height) of the regression was 708 m and r = 0.78. Based on the average effective height, the estimated chemical AOD (AOD = 708 × b_{ext} × 10^{-6}) and SSA contributed by each major component in $PM_{2.5}$ were entered into the TUV model to calculate the DRF at the Earth's surface. The estimated average DRF ranged from -33.2 to -3.4 W m^{-2}, with an arithmetic mean ± standard deviation of -16.5 ± 6.7 W m^{-2} for the campaign. The average DRF for our study is similar to the -13.7 W m^{-2} calculated for photosynthetically active radiation at Xianghe, China in autumn using the Santa Barbara DISORT Atmospheric Radiative Transfer model (SBDART) (Xia et al., 2007a). Further comparisons with previous estimates of DRFs in China at ultraviolet and visible wavelengths show that the average value from our study is similar to that at the rural site of Taihu (-17.8 W m^{-2}, Xia et al., 2007b) but it was less negative than at the suburban or urban sites of Linan (-73.5 W m^{-2}, Xu et al., 2003), Nanjing (-39.4 W m^{-2}, Zhuang et al., 2014), or Xi'an (-100.5 W m^{-2}, Wang et al., 2016b). The more negative DRF values correspond with high aerosol loadings during those studies.

The estimated average DRF during the NCCPC-control period was -14.0 ± 3.0 W m^{-2}, which was less negative than the value during the non-control period (-19.3 ± 8.6 W m^{-2}) (Figure 10b), and this is consistent with lower $PM_{2.5}$ mass loadings during the NCCPC-control period. Even though the DRF values were as high as -24.7 and -28.2 W m^{-2} during PE1 and PE2, respectively, the percent reduction in DRF during the NCCPC-control period versus the non-control period (26.3%) was smaller than the value during the APEC-control study (61.3%, Zhou et al., 2017). Figure 10b also indicates that EC was responsible for the largest (most negative) DRF effects at the surface during the non-control period; the EC DRF value of -13.4 W m^{-2} was followed by OM (-3.0 W m^{-2}), NH_4NO_3 (-2.2 W m^{-2}), $(NH_4)_2SO_4$ (-0.5 W m^{-2}), and fine soil (-0.15 W m^{-2}). The high EC DRF may have been due in part to EC particles

删除的内容: is …as followed by OM (33.3%), EC (16.2%), $(NH_4)_2SO_4$ (11.9%), and fine soil (1.9%). The contributions of the various $PM_{2.5}$ components to b_{ext} were Compared with previous Olympics and APEC studies, …ifferent compared with previous studies of the pollution controls for the Olympics and APECcontributions of $PM_{2.5}$ components to b_{ext} are found… For example, Li et al. (2013) have…reported that $(NH_4)_2SO_4$ (41%) has …ad the largest contribution to b_{ext} during the Olympics, followed by NH_4NO_3 (23%), OM (17%), and EC (9%); Zhou et al. (2017) have …ound that OM (49%) is …as the largest contributor to b_{ext} during the APEC summit, followed by NH_4NO_3 (19%), $(NH_4)_2SO_4$ (13%), and EC (12%). These differences may be attributed to variable efficiencies of the controls for the specific fine particlethe different reductions in $PM_{2.5}$ chemical…species and the …o variations in variable …H among studies, the latter of which can influence the hygroscopic properties of ... [51]

删除的内容: S8…11, the AODs measured with a sunphotometer were well correlateds well…with the b_{ext} under ambient conditions, … with a…he slope (effective height) of the regression was 708 m and r = 0.78. Based on the average effective height, the estimated chemical AOD (AOD = 708 × b_{ext} × 10^{-6}) and SSA contributed by each major component in $PM_{2.5}$ were putted …ntered into the TUV model to calculate their…DRF at the Earth's surface. The estimated average DRF varies …anged from -33.2 to -3.4 W m^{-2}, with an arithmetic mean ± standard deviationaverage…of -16.5 ± 6.7 W m^{-2} during …or the entire …ampaign, … and t…he average DRF for our studyvalue…is similar to the previous study of …13.7 W m^{-2} calculated for photosynthetically active radiation at Xianghe, China in autumn using which is estimated by…the Santa Barbara DISORT Atmospheric Radiative Transfer model (SBDART) in Xianghe in autumn…(Xia et al., 2007a). Further comparisonsCompared…with ... [52]

删除的内容: As shown in Figure 10b, t…he estimated average DRF during the NCCPC …CCPC-control period is …as -14.0 ± 3.0 W m^{-2}, which is …as less negative than the value during the non-control period (-19.3 ± 8.6 W m^{-2}) (Figure 10b), and.…tT…is should be…s consistent with attributed to the…lower $PM_{2.5}$ mass loadings during the NCCPC …CCPC-control period. Even though tT…e DRF reduction ratio…alues were as high as -24.7 and -28.2 W m^{-2} during PE1 and PE2, respectively, the percent reduction in DRF (26.3%)…during the NCCPC …CCPC-control period versus the non-control period (26.3%) wasis…smaller than the value during the APEC-control study period…(61.3%, Zhou et al., 2017). Furthermore, the DRF values can be as high as -24.7 and -28.2 W m^{-2} during the PE1 and PE2, respectively. …igure 10b also shows …ndicates that the DRF caused by different types of chemical components in $PM_{2.5}$. …C has …as responsible for the largest (most ... [53]

internally mixed with other materials because mixing can amplify light absorption and thereby increase DRF. The lower aerosol loadings during the NCCPC-control period can explain why the DRF values for EC, NH_4NO_3, OM, and fine soil in the uncontrolled period were smaller in magnitude -10.1, -1.7, -1.6, and -0.09 W m^{-2}, respectively, than in the non-control period; these were equivalent to decreases of 24.6, 22.7, 46.7, and 40.0%. These results suggest that the short-term mitigation measures implemented during the NCCPC reduced the cooling effects of $PM_{2.5}$ at the surface in Beijing.

4 Conclusions

We investigated the effects of pollution controls put in place during the 19th NCCPC on the chemical composition of $PM_{2.5}$ and aerosol radiative effects at the Earth's surface. The average mass concentration of $PM_{2.5}$ during the NCCPC-control period was 57.9 ± 9.8 μg m^{-3}, which was 31.2% lower relative to the non-control period (84.1 ± 38.8 μg m^{-3}). The major chemical species, that is, OM, NO_3^-, NH_4^+, EC, and fine soil were lower by 43.1, 20.7, 20.6, 25.0, and 40.8% during the NCCPC-control period, respectively compared with samples taken after the controls were removed. Comparisons for only those days with stable meteorological conditions showed that the control versus non-control differences in $PM_{2.5}$ (43.4%), NO_3^- (25.9%), OM (68.1%), EC (40.0%), and fine soil (58.7%) were larger compared with those for all days. Overall, these results indicate that control measures were effective in reducing fine particle pollution. Results of a PMF receptor model showed that biomass burning (27.3%) was the largest contributor to $PM_{2.5}$ mass during the non-control period, followed by secondary particle formation (19.5%), industry processes (17.2%), traffic-related emissions (15.4%), mineral dust (12.3%), and coal burning (8.3%). In contrast, secondary processes (37.3%) were the largest contributor to $PM_{2.5}$ mass during the NCCPC-control period, followed by biomass burning (21.6%), traffic-related emissions (14.8%), coal burning (14.1%), mineral dust (6.3%), and industry processes (6.0%). The mass concentrations of $PM_{2.5}$ contributed by traffic-related emissions, biomass burning, industry processes, and mineral dust all were lower during the NCCPC-control period compared with the non-control period. However, there was no significant difference in $PM_{2.5}$ mass from coal burning between these two periods, and a larger $PM_{2.5}$ mass concentration of secondary particles was found for the NCCPC-control period.

There were two pollution episodes (PE1: 25–27 October and PE2: 31 October–1 November) that occurred after the NCCPC, and the average $PM_{2.5}$ mass concentrations during those events (117.5 μg m^{-3} for PE1 and 124.5 μg m^{-3} for PE2) were more than double those when the controls were in place. For PE1, secondary particle formation was the most important source for fine particles, accounting for 54.6% of

删除的内容: Due to the reduction of …erosol loadings during the NCCPC …CCPC-control period can explain why,…the DRF values for caused by …C, NH_4NO_3, OM, and fine soil in the uncontrolled period were smaller in magnitude are decreased to …10.1, -1.7, -1.6, and -0.09 W m^{-2}, respectively, than in the non-control period; these were equivalent to decreases with corresponding reduced proportions …f 24.6, 22.7, 46.7, and 40.0%. These results suggest that the short-term mitigation measures implemented during the NCCPC control period would useful for alleviating ... [54]

删除的内容: In this study, w…e investigated the effectspresent an investigation of the impacts…of pollutionshort-term emission…controls put in place during the 19th NCCPC on the changes of $PM_{2.5}$ …hemical composition of $PM_{2.5}$ and aerosol radiative effects at the Earth's surface during the 19th NCCPC period… The average mass concentration of $PM_{2.5}$ during the NCCPC …CCPC-control period is …as 57.9 ± 9.8 μg m^{-3}, which is …as decreased by …1.2% lower relative tocompared with…the non-control period (84.1 ± 38.8 μg m^{-3}). The major chemical species, that is, of…OM, NO_3^-, NH_4^+, EC, and fine soil are …ere lowerdecreased…by 43.1, 20.7, 20.6, 25.0, and 40.8% during the NCCPC …CCPC-control period compared with the non-control period… respectively compared with samples taken after the controls were removed. Comparisons for only those When considering the …ays with stable meteorological conditions, …showed that the control versus non-control differences in reduction ratios of …$M_{2.5}$ (43.4%), NO_3^- (25.9%), OM (68.1%), EC (40.0%), and fine soil (58.7%) are …ere larger compared with those for all days. Overall, The…hese results indicate that control measures have great…ere effectiveness…in preventing …educing fine particle pollution. Results of Further, the… PMF receptor model shows …howed that the …iomass burning (27.3%) is …as the largest contributor to $PM_{2.5}$ mass during the non-control period, followed by secondary inorganic aerosol…article formation (19.5%), industry processes (17.2%), traffic-related emissions (15.4%), mineral dust (12.3%), and coal burning (8.3%). In contrast, secondary inorganic aerosol…rocesses (37.3%) is …ere the largest contributor to $PM_{2.5}$ mass during the NCCPC-control period, followed by biomass burning (21.6%), traffic-related emissions (14.8%), coal burning (14.1%), mineral dust ... [55]

删除的内容: are …ere two pollution episodes (PE1: 25–27 October and PE2: 31 October–1 November 1… that occurred subsequently …fter the NCCPC, and control period with …he average $PM_{2.5}$ mass concentrations during those events (of …17.5 μg m^{-3} for PE1 and 124.5 μg m^{-3} on PE1 and…or PE2) were more than double those when the controls were in place, respectively… For the …E1, the…secondary inorganic aerosol…article formation is …as the most important source for fine particles, dominant source ... [56]

$PM_{2.5}$ mass. Aerosol NO_3^- showed the largest contribution to $PM_{2.5}$ mass (26.8%), and the high RH during PE1 likely promoted aqueous reactions involving nitrate. In contrast, OM (31.8%) was the most abundant species in $PM_{2.5}$ during the PE2, and the PMF indicated that biomass burning was the largest source, accounting for 36.0% of the $PM_{2.5}$ mass. The WRF-Chem simulation showed that the BTH region contributed 73.6% and 46.9% of $PM_{2.5}$ mass during the PE1 and PE2, respectively. Calculations based on methods developed for the IMPROVE program indicated that OM was the largest contributor (43.5%) to the chemical b_{ext} during the non-control period, followed by NH_4NO_3 (32.4%), EC (14.3%), $(NH_4)_2SO_4$ (7.6%), and fine soil (2.2%). During the NCCPC-control period, NH_4NO_3 accounted for 36.7% of b_{ext}, and that was followed by OM (33.3%), EC (16.2%), $(NH_4)_2SO_4$ (11.9%), and fine soil (1.9%). The TUV model showed that the estimated average DRF (-14.0 ± 3.0 W m^{-2}) at the surface during the NCCPC-control period is 27.5% less negative than in the non-control period (-19.3 ± 8.6 W m^{-2}), and this is consistent with the lower $PM_{2.5}$ loadings during the NCCPC-control period. Furthermore, EC had the largest (most negative) influence on DRF at the surface during the non-control period; the EC DRF value of -13.4 W m^{-2} was followed by OM (-3.0 W m^{-2}), NH_4NO_3 (-2.2 W m^{-2}), $(NH_4)_2SO_4$ (-0.5 W m^{-2}), and fine soil (-0.15 W m^{-2}). The DRF values caused by EC, NH_4NO_3, OM, and fine soil when the controls were in place were lower by -10.1, -1.7, -1.6, and -0.09 W m^{-2}, respectively, compared with the non-control period, and the corresponding percent reductions were 24.6, 22.7, 46.7, and 40.0%. The results suggest that the short-term mitigation measures during the NCCPC-control period were effective in reducing fine particle pollution and those actions also had radiative effects sufficient to affect surface temperature.

删除的内容: , … Aerosolof which the formation of…NO_3^- showedis…the most important due to its…largest contribution to $PM_{2.5}$ mass (26.8%). …), and the hH…gh RH for …uring PE1 likely promoted is in favour of…aqueous reactions involving nitrate reaction… In contrast, OM (31.8%) is …as the most abundant species in $PM_{2.5}$ during the PE2, and the PMF shows …ndicated that biomass burning is …as the largest source that… accounts …ccounting for 36.0% of the $PM_{2.5}$ mass. The WRF-Chem simulation shows …howed that the BTH region contributes ... [57]

删除的内容: B…sed on methods developed for the IMPROVE formula…rogram indicated that,…OM is …as the largest contributor (43.5%) to the chemical b_{ext} during the non-control period, followed by NH_4NO_3 (32.4%), EC (14.3%), $(NH_4)_2SO_4$ (7.6%), and fine soil (2.2%). During the NCCPC …CCPC-control period, NH_4NO_3 is the largest contributor amounting to…ccounted for 36.7% of b_{ext}, and that wasit is…followed by OM (33.3%), EC (16.2%), $(NH_4)_2SO_4$ (11.9%), and fine soil (1.9%). The TUV model shows …howed that the estimated average DRF (-14.0 ± 3.0 W m^{-2}) at the surface during the NCCPC- …ontrol period is 27.5% less negative than in the non-control period (-19.3 ± 8.6 W m^{-2}), and thiswhich…is consistent withattributed to…the lower $PM_{2.5}$ loadings during the NCCPC- …ontrol period. Furthermore, EC has …ad the largest (most negative) influenceeffects…on DRF at the surface during the non-control period, … the EC that is, a …RF value of -13.4 W m^{-2} was,…followed by OM (-3.0 W m^{-2}), NH_4NO_3 (-2.2 W m^{-2}), $(NH_4)_2SO_4$ (-0.5 W m^{-2}), and fine soil (-0.15 W m^{-2}). TDue to the reduction of aerosol loadings during the NCCPC control period, t…e DRF values caused by EC, NH_4NO_3, OM, and fine soil are …hen the controls were in place were lower bydecreased to…-10.1, -1.7, -1.6, and -0.09 W m^{-2}, respectively, compared with the non-control period, and the corresponding reduced …ercent reductions wereproportions of…24.6, 22.7, 46.7, and 40.0%. The results suggest that the short-term mitigation measures during the NCCPC- …ontrol period were effective in reducing fine particle pollution and those actions also had radiative would useful for alleviating the cooling …ffects sufficient to affect of $PM_{2.5}$ at the surface in Beijing ... [58]

Acknowledgments

This work was supported by the National Research Program for Key Issues in Air Pollution Control (DQGG0105) and the National Natural Science Foundation of China (41503118 and 41661144020). The authors are grateful to the staff from Xianghe Atmospheric Observatory for their assistance with field sampling.

References

Amil, N., Latif, M. T., Khan, M. F., and Mohamad, M.: Seasonal variability of $PM_{2.5}$ composition and sources in the Klang Valley urban-industrial environment, Atmos. Chem. Phys., 16, 5357–5381, https://doi.org/10.5194/acp-16-5357-2016, 2016.

Bei, N., Li, G., and Molina, L. T.: Uncertainties in SOA simulations due to meteorological uncertainties in Mexico City during MILAGRO-2006 field campaign, Atmos. Chem. Phys., 12, 11295–11308, https://doi.org/10.5194/acp-16-5357-2016, 2012.

Bei, N., Wu, J., Elser, M., Feng, T., Cao, J., El-Haddad, I., Li, X., Huang, R., Li, Z., Long, X., Xing, L., Zhao, S., Tie, X., Prévôt, A. S. H., and Li, G.: Impacts of meteorological uncertainties on the haze formation in Beijing–Tianjin–Hebei (BTH) during wintertime: a case study, Atmos. Chem. Phys., 17, 14579–14591, https://doi.org/10.5194/acp-17-14579-2017, 2017.

Bukowiecki, N., Hill, M., Gehrig, R., Zwicky, C. N., Lienemann, P., Hegedüs, F., Falkenberg, G., Weingartner, E., and Baltensperger, U.: Trace metals in ambient air: hourly size-segregated mass concentrations determined by synchrotron-XRF, Environ. Sci. Technol., 39, 5754–5762, doi:10.1021/es048089m, 2005.

Canonaco, F., Slowik, J. G., Baltensperger, U., and Prévôt, A. S. H.: Seasonal differences in oxygenated organic aerosol composition: implications for emissions sources and factor analysis, Atmos. Chem. Phys., 15, 6993–7002, https://doi.org/10.5194/acp-15-6993-2015, 2015.

Cao, J. J., Wang, Q. Y., Chow, J. C., Watson, J. G., Tie, X. X., Shen, Z. X., Wang, P., and An, Z. S.: Impacts of aerosol compositions on visibility impairment in Xi'an, China, Atmos. Environ., 59, 559–566, https://doi.org/10.1016/j.atmosenv.2012.05.036, 2012.

Cao, J. J., Lee, S. C., Ho, K. F., Zhang, X. Y., Zou, S. C., Fung, K., Chow, J. C., and Watson, J. G.: Characteristics of carbonaceous aerosol in Pearl River Delta Region, China during 2001 winter period, Atmos. Environ., 37, 1451–1460, https://doi.org/10.1016/S1352-2310(02)01002-6, 2003.

Cao, J. J., Wu, F., Chow, J. C., Lee, S. C., Li, Y., Chen, S. W., An, Z. S., Fung, K. K., Watson, J. G., Zhu, C. S., and Liu, S. X.: Characterization and source apportionment of atmospheric organic and elemental carbon during fall and winter of 2003 in Xi'an, China, Atmos. Chem. Phys., 5, 3127–3137, https://doi.org/10.5194/acp-5-3127-2005, 2005.

Chalbot, M. C., McElroy, B., and Kavouras, I. G.: Sources, trends and regional impacts of fine particulate matter in southern Mississippi valley: significance of emissions from sources in the Gulf of Mexico coast, Atmos. Chem. Phys., 13, 3721–3732, https://doi.org/10.5194/acp-13-3721-2013, 2013.

Chen, J., Li, C., Ristovski, Z., Milic, A., Gu, Y., Islam, M. S., Wang, S., Hao, J., Zhang, H., He, C., Guo, H., Fu, H., Miljevic, B., Morawska, L., Thai, P., Lam, Y. F., Pereira, G., Ding, A., Huang, X., and Dumka, U. C.: A review of biomass burning: Emissions and impacts on air quality, health and climate in China, Sci. Total Environ., 579, 1000–1034, https://doi.org/10.1016/j.scitotenv.2016.11.025, 2017.

Chen, Y., Xie, S. D., Luo, B., and Zhai, C. Z.: Particulate pollution in urban Chongqing of southwest China: Historical trends of variation, chemical characteristics and source apportionment, Sci. Total Environ., 584–585, 523–534, https://doi.org/10.1016/j.scitotenv.2017.01.060, 2017.

Cheung, K., Daher, N., Shafer, M. M., Ning, Z., Schauer, J. J., and Sioutas, C.: Diurnal trends in coarse particulate matter composition in the Los Angeles Basin, J. Environ. Monit., 13, 3277–3287, doi: 10.1039/c1em10296f, 2011.

Chow, J. C., Watson, J. G., Chen, L. W. A., Chang, M. C. O., Robinson, N. F., Trimble, D., and Kohl, S.: The IMPROVE_A Temperature Protocol for Thermal/Optical Carbon Analysis: Maintaining Consistency with a Long-Term Database, J. Air Waste Manage. Assoc., 57, 1014–1023, https://doi.org/10.3155/1047-3289.57.9.1014, 2007.

Draxler, R. R. and Rolph, G. D.: HYSPLIT (HYbrid Single-Particle Lagrangian Integrated Trajectory), Silver Spring, MD, Model access via NOAA ARL READY Website: http://www.arl.noaa.gov/ready/hysplit4.htmlNOAAAirResourcesLaboratory (last access: February 2018), 2003

删除的内容：Bei, N., Xiao, B., Meng, N., and Feng, T.: Critical role of meteorological conditions in a persistent haze episode in the Guanzhong basin, China, Sci. Total Environ., 550, 273–284, https://doi.org/10.1016/j.scitotenv.2015.12.159, 2016.

Du, H., Kong, L., Cheng, T., Chen, J., Du, J., Li, L., Xia, X., Leng, C., and Huang, G.: Insights into summertime haze pollution events over Shanghai based on online water-soluble ionic composition of aerosols, Atmos. Environ., 45, 5131–5137, https://doi.org/10.1016/j.atmosenv.2011.06.027, 2011.
Duan, J., and Tan, J.: Atmospheric heavy metals and Arsenic in China: Situation, sources and control policies, Atmos. Environ., 74, 93–101, https://doi.org/10.1016/j.atmosenv.2013.03.031, 2013.
Elser, M., Huang, R. J., Wolf, R., Slowik, J. G., Wang, Q. Y., Canonaco, F., Li, G., Bozzetti, C., Daellenbach, K. R., Huang, Y., Zhang, R., Li, Z., Cao, J., Baltensperger, U., El-Haddad, I., and Prévôt, A. S. H.: New insights into $PM_{2.5}$ chemical composition and sources in two major cities in China during extreme haze events using aerosol mass spectrometry, Atmos. Chem. Phys., 16, 3207–3225, https://doi.org/10.5194/acp-16-3207-2016, 2016.
Emmons, L. K., Walters, S., Hess, P. G., Lamarque, J. F., Pfister, G. G., Fillmore, D., Granier, C., Guenther, A., Kinnison, D., Laepple, T., Orlando, J., Tie, X., Tyndall, G., Wiedinmyer, C., Baughcum, S. L., and Kloster, S.: Description and evaluation of the Model for Ozone and Related chemical Tracers, version 4 (MOZART-4), Geosci. Model Dev., 3, 43–67, https://doi.org/10.5194/gmd-3-43-2010, 2010.
Feng, S. L., Gao, D., Liao, F., Zhou, F. R., and Wang, X. M.: The health effects of ambient $PM_{2.5}$ and potential mechanisms, Ecotox. Environ. Safe., 128, 67–74, https://doi.org/10.1016/j.ecoenv.2016.01.030, 2016.
Gao, Y., Liu, X., Zhao, C., and Zhang, M.: Emission controls versus meteorological conditions in determining aerosol concentrations in Beijing during the 2008 Olympic Games, Atmos. Chem. Phys., 11, 12437–12451, https://doi.org/10.5194/acp-11-12437-2011, 2011.
Guo, S., Hu, M., Guo, Q., Zhang, X., Schauer, J. J., and Zhang, R.: Quantitative evaluation of emission controls on primary and secondary organic aerosol sources during Beijing 2008 Olympics, Atmos. Chem. Phys., 13, 8303–8314, https://doi.org/10.5194/acp-13-8303-2013, 2013.
Hallquist, M., Wenger, J. C., Baltensperger, U., Rudich, Y., Simpson, D., Claeys, M., Dommen, J., Donahue, N. M., George, C., Goldstein, A. H., Hamilton, J. F., Herrmann, H., Hoffmann, T., Iinuma, Y., Jang, M., Jenkin, M. E., Jimenez, J. L., Kiendler-Scharr, A., Maenhaut, W., McFiggans, G., Mentel, T. F., Monod, A., Prévôt, A. S. H., Seinfeld, J. H., Surratt, J. D., Szmigielski, R., and Wildt, J.: The formation, properties and impact of secondary organic aerosol: current and emerging issues, Atmos. Chem. Phys., 9, 5155–5236, https://doi.org/10.5194/acp-9-5155-2009, 2009.
Han, X., Guo, Q., Liu, C., Strauss, H., Yang, J., Hu, J., Wei, R., Tian, L., Kong, J., and Peters, M.: Effect of the pollution control measures on $PM_{2.5}$ during the 2015 China Victory Day Parade: Implication from water-soluble ions and sulfur isotope, Environ. Pollut., 218, 230–241, https://doi.org/10.1016/j.envpol.2016.06.038, 2016.
Hsu, S.-C., Liu, S. C., Huang, Y.-T., Chou, C. C. K., Lung, S. C. C., Liu, T.-H., Tu, J.-Y., and Tsai, F.: Long-range southeastward transport of Asian biosmoke pollution: Signature detected by aerosol potassium in Northern Taiwan, J. Geophys. Res.-Atmos., 114, D14301, doi:10.1029/2009JD011725, 2009.
Huang, X., Liu, Z., Liu, J., Hu, B., Wen, T., Tang, G., Zhang, J., Wu, F., Ji, D., Wang, L., and Wang, Y.: Chemical characterization and source identification of $PM_{2.5}$ at multiple sites in the Beijing-Tianjin-Hebei region, China, Atmos. Chem. Phys., 17, 12941–12962, https://doi.org/10.5194/acp-17-12941-2017, 2017.
Khan, M. F., Sulong, N. A., Latif, M. T., Nadzir, M. S. M., Amil, N., Hussain, D. F. M., Lee, V., Hosaini, P. N., Shaharom, S., Yusoff, N. A. Y. M., Hoque, H. M. S., Chung, J. X., Sahani, M., Mohd Tahir, N., Juneng, L., Maulud, K. N. A., Abdullah, S. M. S., Fujii, Y., Tohno, S., and Mizohata, A.: Comprehensive assessment of PM2.5 physicochemical properties during the Southeast Asia dry

869 season (southwest monsoon), J. Geophys. Res.-Atmos., 121, 14589–14611,
870 doi:10.1002/2016JD025894, 2016a.
871 Khan, M. F., Latif, M. T., Saw, W. H., Amil, N., Nadzir, M. S. M., Sahani, M., Tahir, N. M., and Chung,
872 J. X.: Fine particulate matter in the tropical environment: monsoonal effects, source apportionment,
873 and health risk assessment, Atmos. Chem. Phys., 16, 597–617, https://doi.org/10.5194/acp-16-597-
874 2016, 2016b.
875 Kuang, B. Y., Lin, P., Huang, X. H. H., and Yu, J. Z.: Sources of humic-like substances in the Pearl River
876 Delta, China: positive matrix factorization analysis of $PM_{2.5}$ major components and source markers,
877 Atmos. Chem. Phys., 15, 1995–2008, https://doi.org/10.5194/acp-15-1995-2015, 2015.
878 Lecoeur, E., Seigneur, C., Page, C., and Terray, L.: A statistical method to estimate $PM_{2.5}$ concentrations
879 from meteorology and its application to the effect of climate change, J. Geophys. Res.-Atmos., 119,
880 3537–3585, doi:10.1002/2013JD021172, 2014.
881 Li, G., Bei, N., Tie, X., and Molina, L. T.: Aerosol effects on the photochemistry in Mexico City during
882 MCMA-2006/MILAGRO campaign, Atmos. Chem. Phys., 11, 5169–5182,
883 https://doi.org/10.5194/acp-11-5169-2011, 2011a.
884 Li, G., Zavala, M., Lei, W., Tsimpidi, A. P., Karydis, V. A., Pandis, S. N., Canagaratna, M. R., and Molina,
885 L. T.: Simulations of organic aerosol concentrations in Mexico City using the WRF-CHEM model
886 during the MCMA-2006/MILAGRO campaign, Atmos. Chem. Phys., 11, 3789–3809,
887 https://doi.org/10.5194/acp-11-3789-2011, 2011b.
888 Li, G., Lei, W., Bei, N., and Molina, L. T.: Contribution of garbage burning to chloride and $PM_{2.5}$ in
889 Mexico City, Atmos. Chem. Phys., 12, 8751–8761, https://doi.org/10.5194/acp-12-8751-2012, 2012.
890 Li, J., Xie, S. D., Zeng, L. M., Li, L. Y., Li, Y. Q., and Wu, R. R.: Characterization of ambient volatile
891 organic compounds and their sources in Beijing, before, during, and after Asia-Pacific Economic
892 Cooperation China 2014, Atmos. Chem. Phys., 15, 7945–7959, https://doi.org/10.5194/acp-15-
893 7945-2015, 2015.
894 Li, J., and Han, Z.: A modeling study of severe winter haze events in Beijing and its neighboring regions,
895 Atmos. Res., 170, 87–97, https://doi.org/10.1016/j.atmosres.2015.11.009, 2016.
896 Li, X., He, K., Li, C., Yang, F., Zhao, Q., Ma, Y., Cheng, Y., Ouyang, W., and Chen, G.: $PM_{2.5}$ mass,
897 chemical composition, and light extinction before and during the 2008 Beijing Olympics, J. Geophys.
898 Res.-Atmos., 118, 12158–12167, doi:10.1002/2013JD020106, 2013.
899 Liang, P., Zhu, T., Fang, Y., Li, Y., Han, Y., Wu, Y., Hu, M., and Wang, J.: The role of meteorological
900 conditions and pollution control strategies in reducing air pollution in Beijing during APEC 2014
901 and Victory Parade 2015, Atmos. Chem. Phys., 17, 13921–13940, https://doi.org/10.5194/acp-17-
902 13921-2017, 2017.
903 Lim, H.-J., and Turpin, B. J.: Origins of primary and secondary organic aerosol in Atlanta: Results of
904 time-resolved measurements during the Atlanta Supersite Experiment, Environ. Sci. Technol., 36,
905 4489–4496, doi:10.1021/es0206487, 2002.
906 Lin, H., Liu, T., Fang, F., Xiao, J., Zeng, W., Li, X., Guo, L., Tian, L., Schootman, M., Stamatakis, K. A.,
907 Qian, Z., and Ma, W.: Mortality benefits of vigorous air quality improvement interventions during
908 the periods of APEC Blue and Parade Blue in Beijing, China, Environ. Pollut., 220, 222–227,
909 https://doi.org/10.1016/j.envpol.2016.09.041, 2017.
910 Lin, Y. C., Tsai, C. J., Wu, Y. C., Zhang, R., Chi, K. H., Huang, Y. T., Lin, S. H., and Hsu, S. C.:
911 Characteristics of trace metals in traffic-derived particles in Hsuehshan Tunnel, Taiwan: size
912 distribution, potential source, and fingerprinting metal ratio, Atmos. Chem. Phys., 15, 4117–4130,
913 https://doi.org/10.5194/acp-15-4117-2015, 2015.
914 Liu, B., Wu, J., Zhang, J., Wang, L., Yang, J., Liang, D., Dai, Q., Bi, X., Feng, Y., Zhang, Y., and Zhang,
915 Q.: Characterization and source apportionment of $PM_{2.5}$ based on error estimation from EPA PMF

5.0 model at a medium city in China, Environ. Pollut., 222, 10–22, https://doi.org/10.1016/j.envpol.2017.01.005, 2017.
Madronich, S.: UV radiation in the natural and perturbed atmosphere, In: M. Tevini, Ed., *UV-B Radiation and Ozone Depletion*, Lewis Publisher, Boca Raton, 1993.
Malm William, C., Day Derek, E., Kreidenweis Sonia, M., Collett Jeffrey, L., and Lee, T.: Humidity-dependent optical properties of fine particles during the Big Bend Regional Aerosol and Visibility Observational Study, J. Geophys. Res.-Atmos., 108(D9), 4279, doi:10.1029/2002JD002998, 2003.
Men, C., Liu, R., Xu, F., Wang, Q., Guo, L., and Shen, Z.: Pollution characteristics, risk assessment, and source apportionment of heavy metals in road dust in Beijing, China, Sci. Total Environ., 612, 138–147, https://doi.org/10.1016/j.scitotenv.2017.08.123, 2018.
Milando, C., Huang, L., and Batterman, S.: Trends in PM2.5 emissions, concentrations and apportionments in Detroit and Chicago, Atmos. Environ., 129, 197–209, https://doi.org/10.1016/j.atmosenv.2016.01.012, 2016.
National Bureau of Statistics (NBS): China Statistical Yearbook 2013, China Statistics Press, Beijing, 2013a (in Chinese).
Norris, G., Duvall, R., Brown, S., and Bai, S.: EPA Positive Matrix Factorization (PMF) 5.0 fundamentals and User Guide Prepared for the US Environmental Protection Agency Office of Research and Development, Washington, DC, Inc., Petaluma, 2014.
Paatero, P., and Tapper, U.: Positive matrix factorization: A non-negative factor model with optimal utilization of error estimates of data values, Environmetrics, 5, 111–126, https://doi.org/10.1002/env.3170050203, 2006.
Palancar, G. G., and Toselli, B. M.: Effects of meteorology and tropospheric aerosols on UV-B radiation: a 4-year study, Atmos. Environ., 38, 2749–2757, https://doi.org/10.1016/j.atmosenv.2004.01.036, 2004.
Pipal, A. S., Kulshrestha, A., and Taneja, A.: Characterization and morphological analysis of airborne $PM_{2.5}$ and PM_{10} in Agra located in north central India, Atmos. Environ., 45, 3621–3630, https://doi.org/10.1016/j.atmosenv.2011.03.062, 2011.
Pitchford, M., Malm, W., Schichtel, B., Kumar, N., Lowenthal, D., and Hand, J.: Revised algorithm for estimating light extinction from IMPROVE particle speciation data, J. Air Waste Manage. Assoc., 57, 1326–1336, doi:10.3155/1047-3289.57.11.1326, 2007.
Pui, D. Y. H., Chen, S. C., and Zuo, Z. L.: $PM_{2.5}$ in China: Measurements, sources, visibility and health effects, and mitigation, Particuology, 13, 1–26, https://doi.org/10.1016/j.partic.2013.11.001, 2014.
Ran, L., Deng, Z. Z., Wang, P. C., and Xia, X. A.: Black carbon and wavelength-dependent aerosol absorption in the North China Plain based on two-year aethalometer measurements, Atmos. Environ., 142, 132–144, https://doi.org/10.1016/j.atmosenv.2016.07.014, 2016.
Sammaritano, M. A., Bustos, D. G., Poblete, A. G., and Wannaz, E. D.: Elemental composition of $PM_{2.5}$ in the urban environment of San Juan, Argentina, Environ. Sci. Pollut. Res., 25, 4197–4203, https://doi.org/10.1007/s11356-017-0793-5, 2018.
Sun, Y., Jiang, Q., Wang, Z., Fu, P., Li, J., Yang, T., and Yin, Y.: Investigation of the sources and evolution processes of severe haze pollution in Beijing in January 2013, J. Geophys. Res.-Atmos., 119, 4380–4398, doi:10.1002/2014JD021641, 2014.
Tang, G., Zhu, X., Hu, B., Xin, J., Wang, L., Münkel, C., Mao, G., and Wang, Y.: Impact of emission controls on air quality in Beijing during APEC 2014: lidar ceilometer observations, Atmos. Chem. Phys., 15, 12667–12680, https://doi.org/10.5194/acp-15-12667-2015, 2015.
Tao, J., Gao, J., Zhang, L., Zhang, R., Che, H., Zhang, Z., Lin, Z., Jing, J., Cao, J., and Hsu, S. C.: $PM_{2.5}$ pollution in a megacity of southwest China: source apportionment and implication, Atmos. Chem. Phys., 14, 8679–8699, https://doi.org/10.5194/acp-14-8679-2014, 2014.

删除的内容：
Massabò, D., Caponi, L., Bernardoni, V., Bove, M. C., Brotto, P., Calzolai, G., Cassola, F., Chiari, M., Fedi, M. E., Fermo, P., Giannoni, M., Lucarelli, F., Nava, S., Piazzalunga, A., Valli, G., Vecchi, R., and Prati, P.: Multi-wavelength optical determination of black and brown carbon in atmospheric aerosols, Atmos. Environ., 108, 1–12, https://doi.org/10.1016/j.atmosenv.2015.02.058, 2015.

删除的内容：Park, S. H., Gong, S. L., Bouchet, V. S., Gong, W., Makar, P. A., Moran, M. D., Stroud, C. A., and Zhang, J.: Effects of black carbon aging on air quality predictions and direct radiative forcing estimation, Tellus Ser. B-Chem. Phys. Meteorol., 63, 1026–1039, https://doi.org/10.1111/j.1600-0889.2011.00558.x, 2011.

Tao, J., Gao, J., Zhang, L., Wang, H., Qiu, X., Zhang, Z., Wu, Y., Chai, F., and Wang, S.: Chemical and optical characteristics of atmospheric aerosols in Beijing during the Asia-Pacific Economic Cooperation China 2014, Atmos. Environ., 144, 8–16, https://doi.org/10.1016/j.atmosenv.2016.08.067, 2016.

Tao, J., Zhang, L. M., Cao, J. J., and Zhang, R. J.: A review of current knowledge concerning $PM_{2.5}$ chemical composition, aerosol optical properties and their relationships across China, Atmos. Chem. Phys., 17, 9485–9518, https://doi.org/10.5194/acp-17-9485-2017, 2017.

Tie, X., Huang, R.-J., Dai, W., Cao, J., Long, X., Su, X., Zhao, S., Wang, Q., and Li, G.: Effect of heavy haze and aerosol pollution on rice and wheat productions in China, Sci. Rep., 6, 29612, doi:10.1038/srep29612, 2016.

Wang, J., Wang, G., Gao, J., Wang, H., Ren, Y., Li, J., Zhou, B., Wu, C., Zhang, L., Wang, S., and Chai, F.: Concentrations and stable carbon isotope compositions of oxalic acid and related SOA in Beijing before, during, and after the 2014 APEC, Atmos. Chem. Phys., 17, 981–992, https://doi.org/10.5194/acp-17-981-2017, 2017.

Wang, Q. Q., He, X., Huang, X. H. H., Griffith, S. M., Feng, Y., Zhang, T., Zhang, Q., Wu, D., and Yu, J. Z.: Impact of Secondary organic aerosol tracers on tracer-based source apportionment of organic carbon and $PM_{2.5}$: A case study in the Pearl River Delta, China, Earth and Space Chemistry, 1, 562–571, doi:10.1021/acsearthspacechem.7b00088, 2017.

Wang, Q. Y., Huang, R.-J., Cao, J., Tie, X., Shen, Z., Zhao, S., Han, Y., Li, G., Li, Z., Ni, H., Zhou, Y., Wang, M., Chen, Y., and Su, X.: Contribution of regional transport to the black carbon aerosol during winter haze period in Beijing, Atmos. Environ., 132, 11–18, http://dx.doi.org/10.1016/j.atmosenv.2016.02.031, 2016a.

Wang, Q. Y., Huang, R.-J., Zhao, Z., Cao, J., Ni, H., Tie, X., Zhao, S., Su, X., Han, Y., Shen, Z., Wang, Y., Zhang, N., Zhou, Y., and Corbin, J. C.: Physicochemical characteristics of black carbon aerosol and its radiative impact in a polluted urban area of China, J. Geophys. Res.-Atmos., 121, 12505–12519, doi:10.1002/2016JD024748, 2016b.

Wang, Q. Y., Cao, J., Han, Y., Tian, J., Zhang, Y., Pongpiachan, S., Zhang, Y., Li, L., Niu, X., Shen, Z., Zhao, Z., Tipmanee, D., Bunsomboonsakul, S., Chen, Y., and Sun, J.: Enhanced light absorption due to the mixing state of black carbon in fresh biomass burning emissions, Atmos. Environ., 180, 184–191, https://doi.org/10.1016/j.atmosenv.2018.02.049, 2018a.

Wang, Q. Y., Cao, J., Han, Y., Tian, J., Zhu, C., Zhang, Y., Zhang, N., Shen, Z., Ni, H., Zhao, S., and Wu, J.: Sources and physicochemical characteristics of black carbon aerosol from the southeastern Tibetan Plateau: internal mixing enhances light absorption, Atmos. Chem. Phys., 18, 4639–4656, https://doi.org/10.5194/acp-18-4639-2018, 2018b.

Wang, S., Zhao, M., Xing, J., Wu, Y., Zhou, Y., Lei, Y., He, K., Fu, L., and Hao, J.: Quantifying the Air Pollutants Emission Reduction during the 2008 Olympic Games in Beijing, Environ. Sci. Technol., 44, 2490–2496, doi:10.1021/es9028167, 2010.

Wang, W., Primbs, T., Tao, S., and Simonich, S. L. M.: Atmospheric particulate matter pollution during the 2008 Beijing Olympics, Environ. Sci. Technol., 43, 5314–5320, doi:10.1021/es9007504, 2009.

Wang, Z., Li, Y., Chen, T., Li, L., Liu, B., Zhang, D., Sun, F., Wei, Q., Jiang, L., and Pan, L.: Changes in atmospheric composition during the 2014 APEC conference in Beijing, J. Geophys. Res.-Atmos., 120, 12695–12707, doi:10.1002/2015JD023652, 2015.

Watson, J. G.: Visibility: Science and regulation, J. Air Waste Manage. Assoc., 52, 628–713, https://doi.org/10.1080/10473289.2002.10470813, 2002.

Xia, X., Li, Z., Wang, P., Chen, H., and Cribb, M.: Estimation of aerosol effects on surface irradiance based on measurements and radiative transfer model simulations in northern China, J. Geophys. Res.- Atmos., 112, D22S10, doi:10.1029/2006JD008337, 2007a.

删除的内容：Tao, J., Zhang, L., Gao, J., Wang, H., Chai, F., and Wang, S.: Aerosol chemical composition and light scattering during a winter season in Beijing, Atmos. Environ., 110, 36–44, https://doi.org/10.1016/j.atmosenv.2015.03.037, 2015.

Xia, X., Li, Z, Holben, B., Wang, P., Eck, T., Chen, H., Cribb, M., and Zhao, Y.: Aerosol optical properties and radiative effects in the Yangtze Delta region of China, J. Geophys. Res.- Atmos., 112, D22S12, doi:10.1029/2007JD008859, 2007b.

Xiao, S., Wang, Q., Cao, J., Huang, R.-J., Chen, W., Han, Y., Xu, H., Liu, S., Zhou, Y., and Wang, P.: Long-term trends in visibility and impacts of aerosol composition on visibility impairment in Baoji, China, Atmos. Res., 149, 88–95, http://dx.doi.org/10.1016/j.atmosres.2014.06.006, 2014.

Xie, R., Sabel, C. E., Lu, X., Zhu, W. M., Kan, H. D., Nielsen, C. P., and Wang, H. K.: Long-term trend and spatial pattern of $PM_{2.5}$ induced premature mortality in China, Environ. Int., 97, 180–186, https://doi.org/10.1016/j.envint.2016.09.003, 2016.

Xu, H. M., Cao, J. J., Ho, K. F., Ding, H., Han, Y. M., Wang, G. H., Chow, J. C., Watson, J. G., Khol, S. D., Qiang, J., and Li, W. T.: Lead concentrations in fine particulate matter after the phasing out of leaded gasoline in Xi'an, China, Atmos. Environ., 46, 217–224, https://doi.org/10.1016/j.atmosenv.2011.09.078, 2012.

Xu, J., Bergin, M. H., and Greenwald, R.: Direct aerosol radiative forcing in the Yangtze delta region of China: Observation and model estimation, J. Geophys. Res.-Atmos., 108(D2), 4060, doi:10.1029/2002JD002550, 2003.

Xu, W., Song, W., Zhang, Y., Liu, X., Zhang, L., Zhao, Y., Liu, D., Tang, A., Yang, D., Wang, D., Wen, Z., Pan, Y., Fowler, D., Collett Jr, J. L., Erisman, J. W., Goulding, K., Li, Y., and Zhang, F.: Air quality improvement in a megacity: implications from 2015 Beijing Parade Blue pollution control actions, Atmos. Chem. Phys., 17, 31–46, https://doi.org/10.5194/acp-17-31-2017, 2017.

Xu, W. Q., Sun, Y. L., Chen, C., Du, W., Han, T. T., Wang, Q. Q., Fu, P. Q., Wang, Z. F., Zhao, X. J., Zhou, L. B., Ji, D. S., Wang, P. C., and Worsnop, D. R.: Aerosol composition, oxidation properties, and sources in Beijing: results from the 2014 Asia-Pacific Economic Cooperation summit study, Atmos. Chem. Phys., 15, 13681–13698, https://doi.org/10.5194/acp-15-13681-2015, 2015.

Yang, M., Howell, S. G., Zhuang, J., and Huebert, B. J.: Attribution of aerosol light absorption to black cabon, brown carbon, and dust in China–interpertations of atmospheric measurements during EAST-AIRE, Atmos. Chem. Phys., 9, 2035–2050, https://doi.org/10.5194/acp-9-2035-2009, 2009.

Zhang, R., Jing, J., Tao, J., Hsu, S. C., Wang, G., Cao, J., Lee, C. S. L., Zhu, L., Chen, Z., Zhao, Y., and Shen, Z.: Chemical characterization and source apportionment of $PM_{2.5}$ in Beijing: seasonal perspective, Atmos. Chem. Phys., 13, 7053–7074, doi:10.5194/acp-13-7053-2013, 2013.

Zhang, T., Cao, J. J., Tie, X. X., Shen, Z. X., Liu, S. X., Ding, H., Han, Y. M., Wang, G. H., Ho, K. F., Qiang, J., and Li, W. T.: Water-soluble ions in atmospheric aerosols measured in Xi'an, China: Seasonal variations and sources, Atmos. Res., 102, 110–119, https://doi.org/10.1016/j.atmosres.2011.06.014, 2011.

Zhang, Y., Lang, J., Cheng, S., Li, S., Zhou, Y., Chen, D., Zhang, H., and Wang, H.: Chemical composition and sources of PM_1 and $PM_{2.5}$ in Beijing in autumn, Sci. Total Environ., 630, 72–82, https://doi.org/10.1016/j.scitotenv.2018.02.151, 2018.

Zheng, G., Duan, F., Ma, Y., Zhang, Q., Huang, T., Kimoto, T., Cheng, Y., Su, H., and He, K.: Episode-based evolution pattern analysis of haze pollution: Method development and results from Beijing, China, Environ. Sci. Technol., 50, 4632–4641, doi:10.1021/acs.est.5b05593, 2016.

Zheng, G. J., Duan, F. K., Su, H., Ma, Y. L., Cheng, Y., Zheng, B., Zhang, Q., Huang, T., Kimoto, T., Chang, D., Pöschl, U., Cheng, Y. F., and He, K. B.: Exploring the severe winter haze in Beijing: the impact of synoptic weather, regional transport and heterogeneous reactions, Atmos. Chem. Phys., 15, 2969–2983, https://doi.org/10.5194/acp-15-2969-2015, 2015.

Zhong, J., Zhang, X., Dong, Y., Wang, Y., Liu, C., Wang, J., Zhang, Y., and Che, H.: Feedback effects of boundary-layer meteorological factors on cumulative explosive growth of $PM_{2.5}$ during winter

heavy pollution episodes in Beijing from 2013 to 2016, Atmos. Chem. Phys., 18, 247–258, https://doi.org/10.5194/acp-18-247-2018, 2018.

Zong, Z., Wang, X., Tian, C., Chen, Y., Qu, L., Ji, L., Zhi, G., Li, J., and Zhang, G.: Source apportionment of $PM_{2.5}$ at a regional background site in North China using PMF linked with radiocarbon analysis: insight into the contribution of biomass burning, Atmos. Chem. Phys., 16, 11249–11265, https://doi.org/10.5194/acp-16-11249-2016, 2016.

Zhou, Y., Wang, Q., Huang, R., Liu, S., Tie, X., Su, X., Niu, X., Zhao, Z., Ni, H., Wang, M., Zhang, Y., and Cao, J.: Optical properties of aerosols and implications for radiative effects in Beijing during the Asia-Pacific Economic Cooperation Summit 2014, J. Geophys. Res.-Atmos., 122, 10119–10132, https://doi.org/10.1002/2017JD026997, 2017.

Zhuang, B. L., Wang, T. J., Liu, J., Li, S., Xie, M., Yang, X. Q., Fu, C. B., Sun, J. N., Yin, C. Q., Liao, J. B., Zhu, J. L., and Zhang, Y.: Continuous measurement of black carbon aerosol in urban Nanjing of Yangtze River Delta, China, Atmos. Environ., 89, 415–424, https://doi.org/10.1016/j.atmosenv.2014.02.052, 2014.

087 **Table 1** Summary of $PM_{2.5}$ and its major chemical components at Xianghe during the 19th
088 National Congress of the Communist Party of China (NCCPC)-control and non-control periods.

Components	Grand average ($\mu g\ m^{-3}$)	Control period ($\mu g\ m^{-3}$)	Non-control period ($\mu g\ m^{-3}$)	Change ratio[a] (%)
$PM_{2.5}$	70.0	57.9 (63.7)[b]	84.1 (112.6)	31.2 (43.4)
NO_3^-	15.0	13.4 (18.0)	16.9 (24.3)	20.7 (25.9)
SO_4^{2-}	5.6	5.8 (7.6)	5.3 (6.6)	-9.4 (-15.2)
NH_4^+	6.0	5.4 (8.6)	6.8 (9.7)	20.6 (11.3)
Cl^-	2.2	1.6 (1.5)	2.9 (3.4)	44.8 (55.9)
Organic matter	18.9	14.0 (9.5)	24.6 (29.8)	43.1 (68.1)
Elemental carbon	5.2	4.5 (4.5)	6.0 (7.5)	25.0 (40.0)
Trace elements	1.8	1.4 (1.2)	2.3 (3.0)	39.1 (60.0)
Fine soil	5.5	4.2 (2.6)	7.1 (6.3)	40.8 (58.7)

089 [a]([Non-control period]-[NCCPC-control period])/[Non-control period].
090 [b]Values in parentheses show the results for days with stable meteorological conditions (wind
091 speed < 0.4 m s^{-1} and mixed layer height < 274 m).
092

Figure Captions

Figure 1. Location of the Xianghe sampling site. The map was drawn using the ArcGIS.

Figure 2. (left) Daily variations in the contributions of chemical species to $PM_{2.5}$ mass during the campaign and (right) average contributions of chemical species during the 19th National Congress of the Communist Party of China (NCCPC)-control and non-control periods. PE1 and PE2 represent two pollution episodes.

Figure 3. Scatter plots showing the relationships between $PM_{2.5}$ mass concentrations and (a) wind speed and (b) mixed layer height.

Figure 4. (a) Source profiles for the six sources identified using the positive matrix factorization model version 5.0, (b) the mass concentrations of $PM_{2.5}$ contributed by each source, and (c) the average source contribution of each source to the $PM_{2.5}$ mass.

Figure 5. Average source contributions of (a) each positive matrix factorization source factor and (b) chemical species to the $PM_{2.5}$ mass during two pollution episodes (PE1 and PE2).

Figure 6. Correlations for (a) $PM_{2.5}$ mass concentrations versus molar ratios of NO_3^- and NO_2 (NOR), (b) NOR versus relative humidity (RH), (c) the ratio of secondary organic aerosol to elemental carbon (SOA/EC) ratios versus Ox (O_3 + NO_2), and (d) SOA/EC versus RH for all samples from the campaign.

Figure 7. Three-day backward in time air mass trajectories (BT) arriving at 150 m above ground every hour from 31 October to 1 November 2017. The orange points represent fire counts that were derived from Moderate Resolution Imaging Spectroradiometer observations.

Figure 8. Surface weather charts for 08:00 (local time) over East Asia from 22 October to 2 November 2017. The black triangles represent Xianghe.

Figure 9. Daily average $PM_{2.5}$ concentrations ($\mu g\ m^{-3}$) simulated for the Beijing-Tianjin-Hebei region and surrounding areas from 25 October to 2 November 2017. The Weather Research and Forecasting model coupled to chemistry (WRF-Chem) model was used for the simulation.

Figure 10. Average values of (a) light extinction coefficients (including light scattering and absorption) and (b) direct radiative forcing (DRF) at the surface contributed by each $PM_{2.5}$ chemical composition during the 19th National Congress of the Communist Party of China (NCCPC)-control and non-control periods.

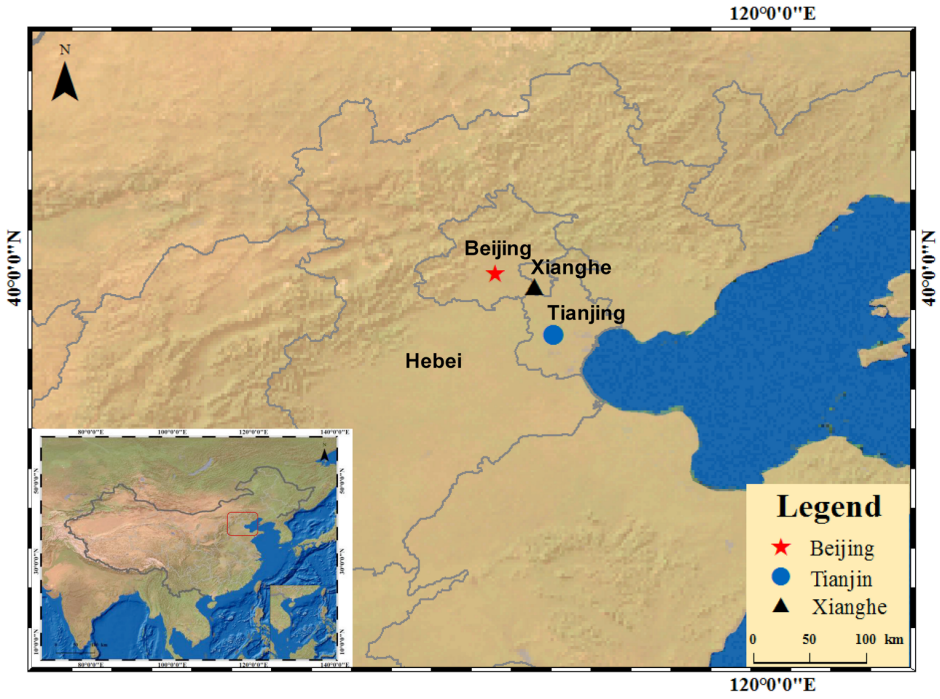
120°0'0"E
N
40°0'0"N
Beijing
Xianghe
Tianjing
Hebei
Legend
Beijing
Tianjin
Xianghe
0
50
100 km
120°0'0"E

Figure 1.

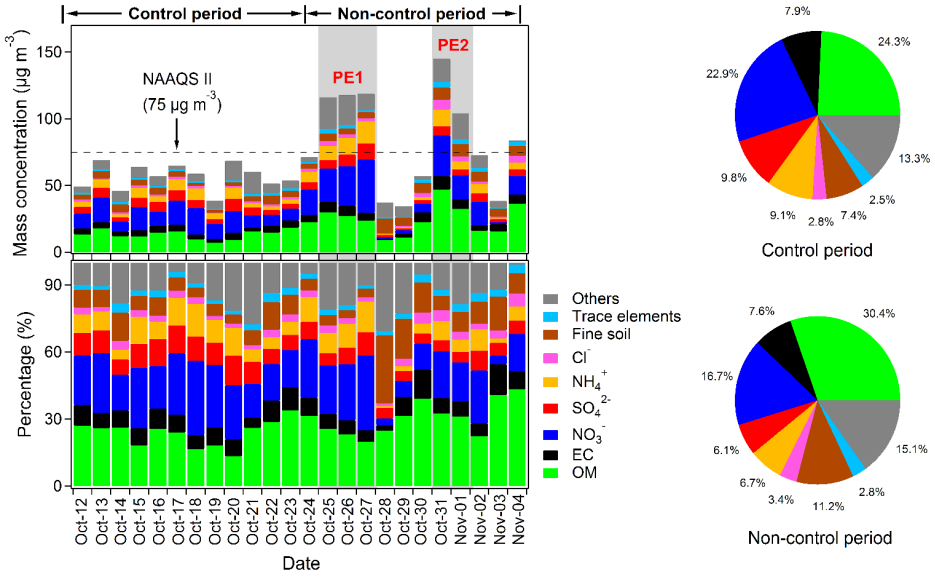
Control period
Non-control period
PE1
PE2
NAAQS II
(75 μg m-3)
Mass concentration (μg m-3)
Percentage (%)
Date
Others
Trace elements
Fine soil
Cl-
NH4+
SO42-
NO3-
EC
OM
7.9%
24.3%
22.9%
13.3%
9.8%
2.5%
9.1%
2.8%
7.4%
Control period
7.6%
30.4%
16.7%
15.1%
6.1%
6.7%
3.4%
11.2%
2.8%
Non-control period

Figure 2.

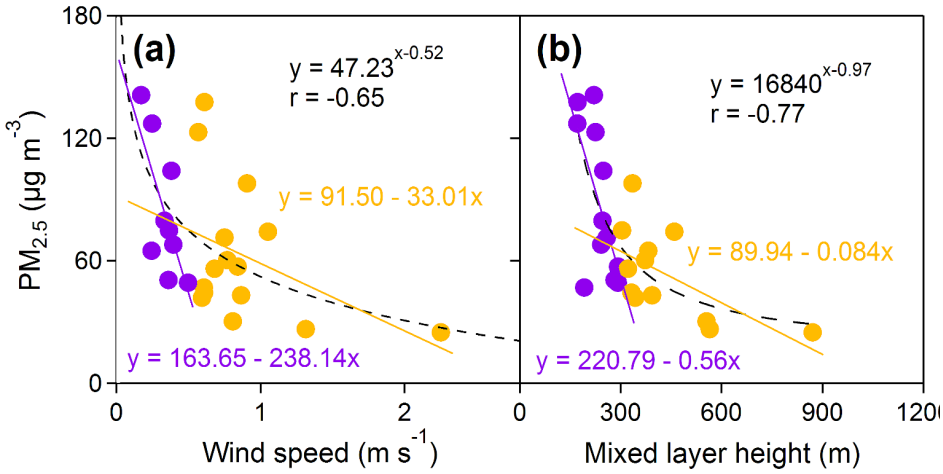

129

130

131 **Figure 3.**

132

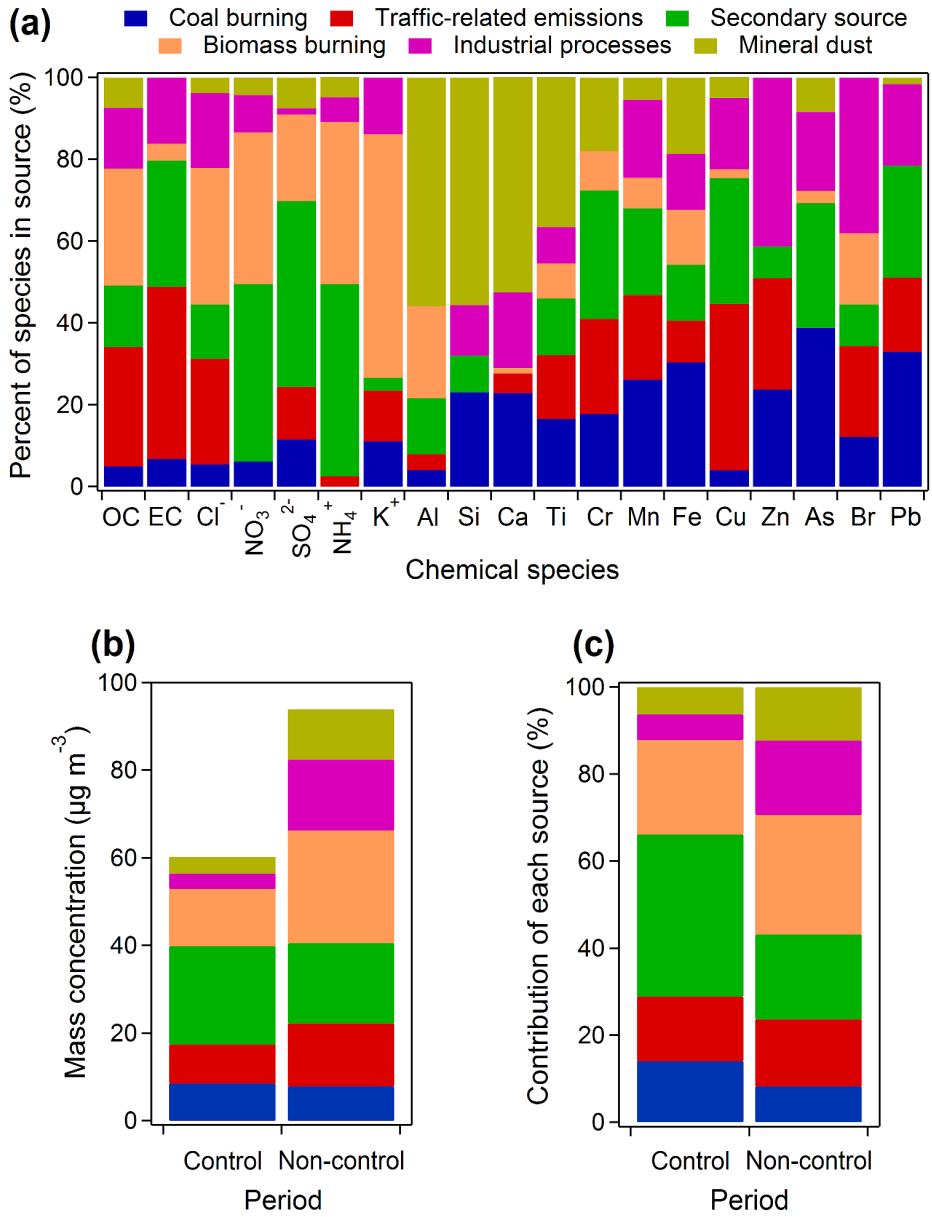
(a)
Coal burning
Traffic-related emissions
Secondary source
Biomass burning
Industrial processes
Mineral dust
Percent of species in source (%)
0
20
40
60
80
100
OC EC Cl⁻ NO3⁻ SO4 2- NH4+ K+ Al Si Ca Ti Cr Mn Fe Cu Zn As Br Pb
Chemical species
(b)
Mass concentration (μg m-3)
0
20
40
60
80
100
Control Non-control
Period
(c)
Contribution of each source (%)
0
20
40
60
80
100
Control Non-control
Period

Figure 4.

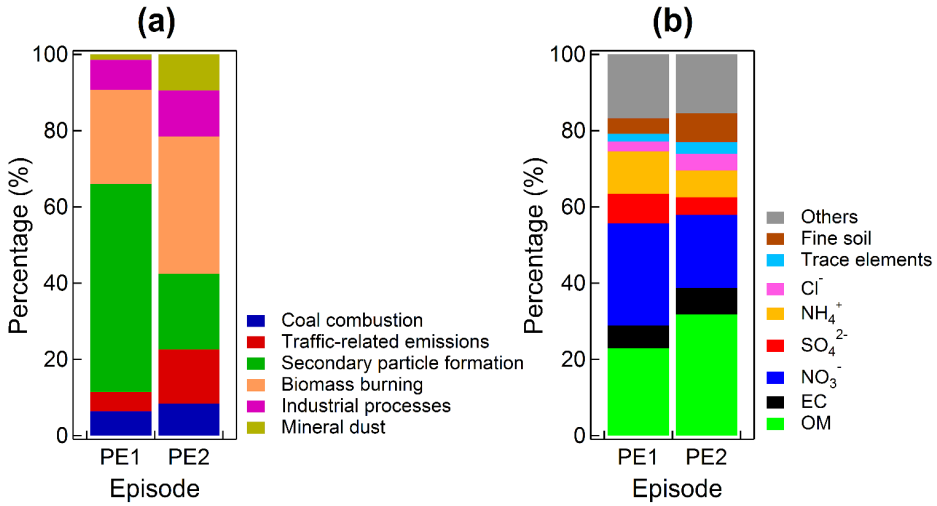

136

137

138 **Figure 5.**

139

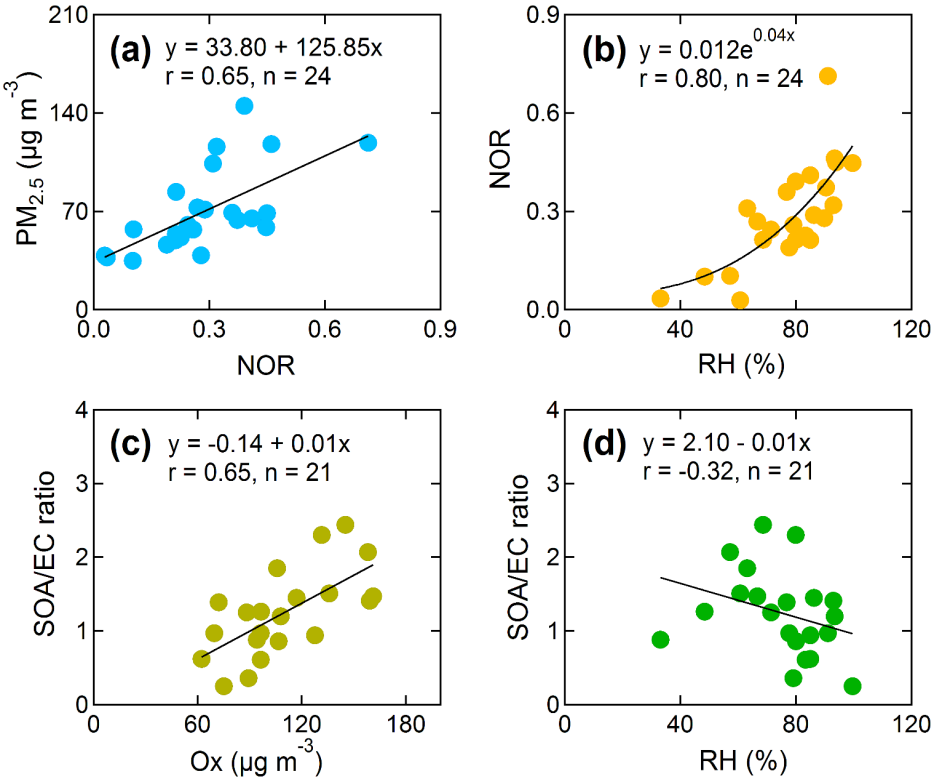

140
141

142 **Figure 6.**

143

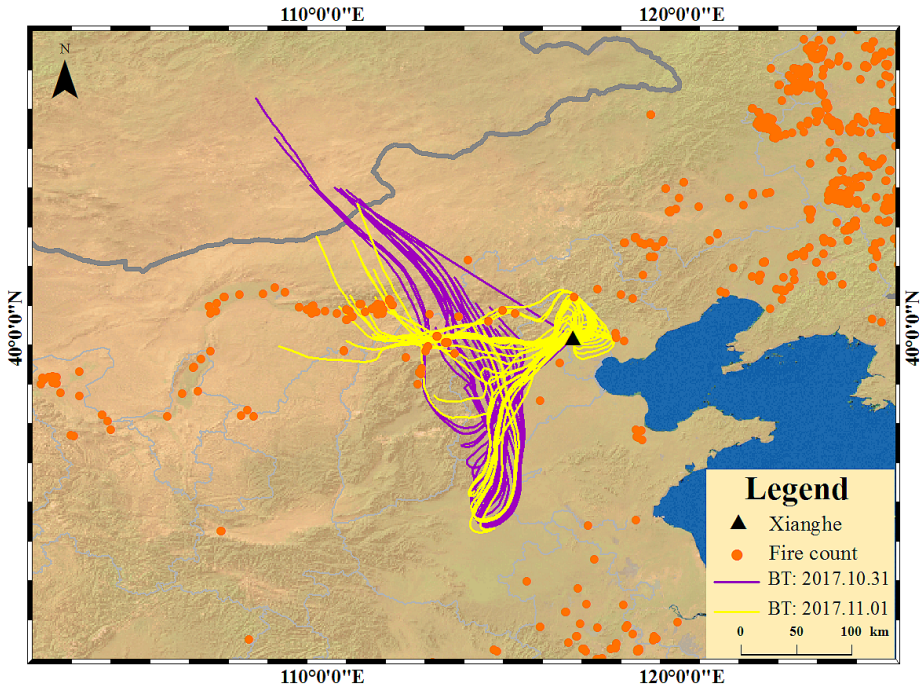
110°0'0"E
120°0'0"E
N
40°0'0"N
Legend
Xianghe
Fire count
BT: 2017.10.31
BT: 2017.11.01
0
50
100 km

Figure 7.

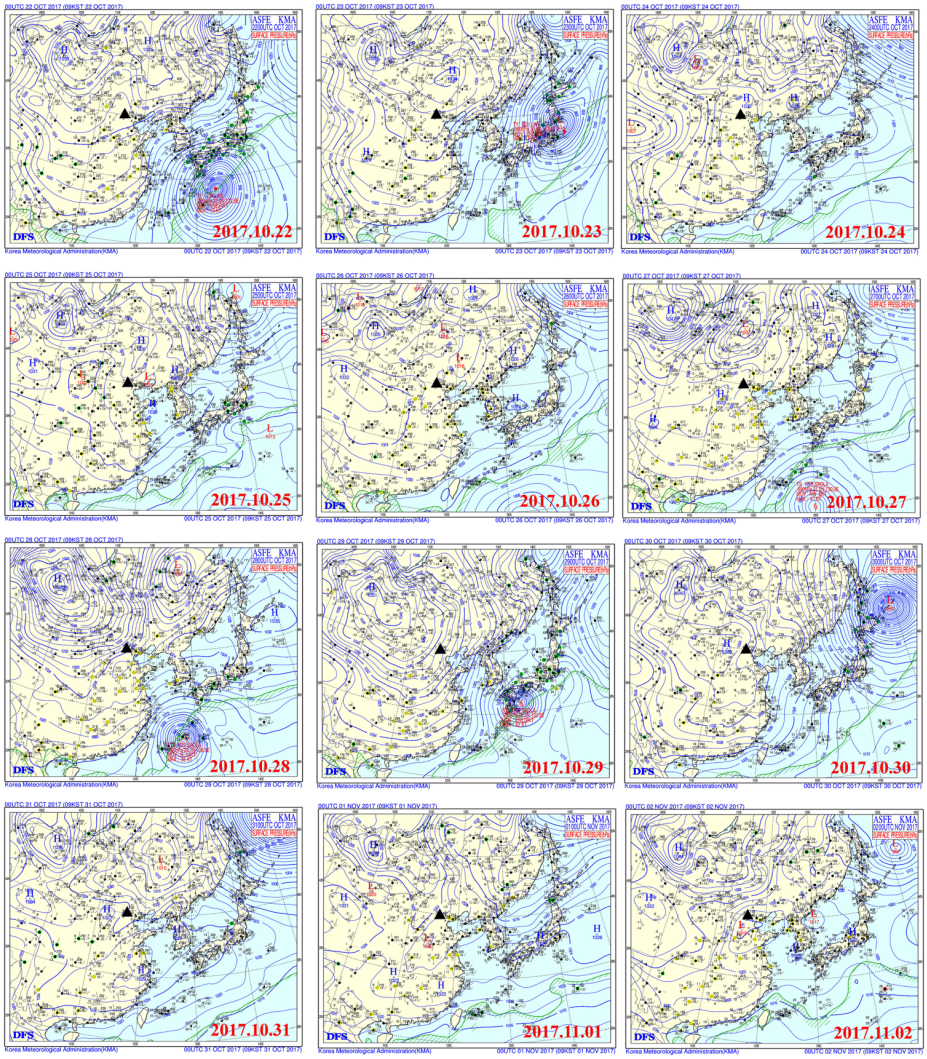
2017.10.22
2017.10.23
2017.10.24
2017.10.25
2017.10.26
2017.10.27
2017.10.28
2017.10.29
2017.10.30
2017.10.31
2017.11.01
2017.11.02

Figure 8.

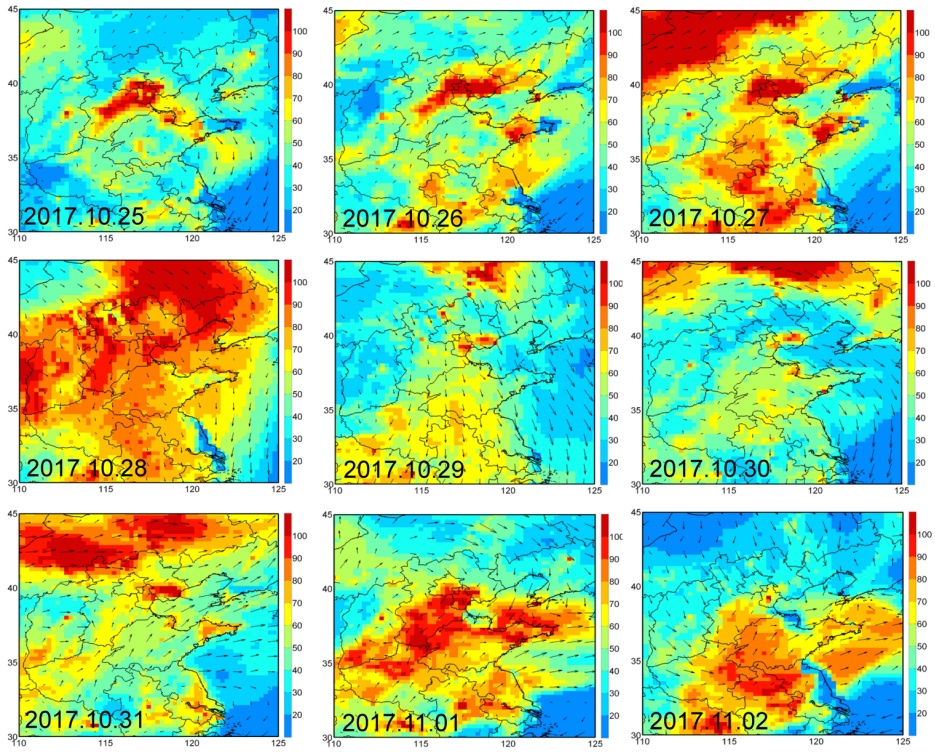
2017.10.25
2017.10.26
2017.10.27
2017.10.28
2017.10.29
2017.10.30
2017.10.31
2017.11.01
2017.11.02

Figure 9.

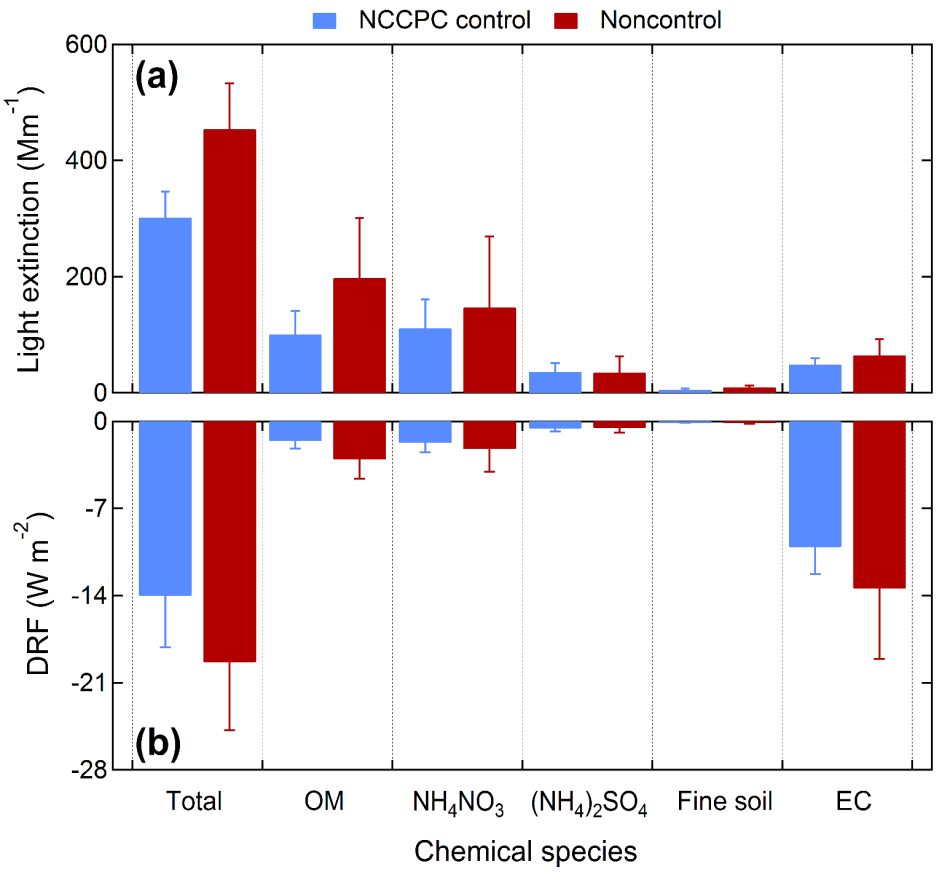

156
157

158 **Figure 10.**